



Surface mass balance projections until 2100 for Folgefonna, a Norwegian ice cap

Rebekka Frøystad^{1,2} and Andreas Born^{1,2}

¹ Department of Earth Science, University of Bergen, Bergen, Norway

² Bjerknes Centre for Climate Research, Bergen, Norway

Correspondence: Rebekka Frøystad (rebekka.froystad@uib.no)

Abstract.

Robust glacier projections are essential for mountain communities adapting to climate change, yet current projections are limited by climate data that either have coarse spatial resolution or span only a narrow range of future scenarios, thereby obscuring the true scale of predictive uncertainty. In this study, we quantify the cascading impact of uncertainty in climate
5 projections on glacier surface mass balance (SMB) projections. We simulate the SMB of the Folgefonna glacier complex in western Norway for 1970–2100 using the energy-balance and snowpack model BESSI. To represent future climate forcing, we use the EURO-CORDEX ensemble, but show that the dataset is systematically too cold and too wet and exhibits unrealistic precipitation patterns for the western Norway region. We therefore develop a downscaling framework in which each EURO-CORDEX member is represented by analogs drawn from a high resolution convection-permitting model (NorCP). This enables
10 SMB projections that account for a plausible spread in climate models and are based on high-resolution climate data with explicitly resolved physical processes. Using this method, we present the most detailed SMB projections of Folgefonna to date for three emission scenarios until 2100. Whether the glacier complex retains any accumulation zone by 2100 depends on the emission scenario. Ensemble medians indicate that Midtfonna loses its accumulation zone in all scenarios, Nordfonna does so in RCP4.5, and no accumulation zone remains on Folgefonna in RCP8.5. However, cumulative SMB (2026–2100) has an
15 uncertainty of 65–75 m w.e. within each scenario due to climate model spread (25th to 75th quantiles). We furthermore find that the choice of global circulation model has a stronger influence on Folgefonna’s SMB than the choice of regional climate model. These findings underscore the need for improving upon agreement between climate models. Detailed glacier mass change projections based on only a subset of the available and hence plausible climate projections underestimate uncertainty and should be considered with caution.



20 1 Introduction

Mountain glaciers and ice caps are retreating worldwide (Hugonnet et al., 2021), changing water supply systems and placing stress on downstream communities. Around 10% of the global population lives in such high-mountain regions severely impacted by climate change (Viviroli et al., 2011). Glacier loss has a multitude of consequences for downstream agriculture, drinking water security, hydropower, and downstream ecosystems (Milner et al., 2017). Making informed adaptation decisions in mountain areas therefore hinges on robust glacier projections that 1) can *accurately* reproduce past climate events, 2) convey a *range* of possible scenarios and their likelihood, and 3) are available at temporal and spatial *resolutions* that are relevant to affected parties and decision-makers.

How a glacier evolves is largely controlled by its surface mass balance (SMB) which describes the glacier's mass budget at the surface and shows how it responds to changes in the climate. Especially in a regime dominated by melt, a realistic representation of the SMB is a prerequisite for making projections on downstream water availability. Positive SMB terms are solid precipitation or water that is retained by the snowpack, while negative ones are mass that is removed typically through runoff, sublimation, or wind erosion. SMB models range from simple positive degree-day (PDD) estimates to models that resolve physical firn processes in high detail (Fettweis et al., 2020; Zekollari et al., 2022).

However, any SMB model is only as good as the climate data forcing it and uncertainty in climate projections will necessarily propagate into SMB projections. While glacier model uncertainty is the greatest source of uncertainty for glacier projections until the middle of the century, climate scenario uncertainty dominates thereafter (Marzeion et al., 2020). In addition to scenario choice, individual climate models typically exhibit a wide spread in their projections due to structural differences between models, especially at small regional scales (Radić et al., 2014; Tebaldi et al., 2021). How climate variability is represented in climate models or included in glacier models also substantially influences glacier projections (Reichert et al., 2002; Farinotti, 2013; Malone et al., 2019; Zolles and Born, 2024). Sources of climate model uncertainty compound and combine so that the dominant source of uncertainty to glacier projections tend to stem from different climate model setups and does not depend as much on, i.e., SMB model parameters (Aschwanden et al., 2019; Holube et al., 2022; Weathers et al., 2025).

Currently, state-of-the-art glacier projections are heavily based on global- and regional-scale studies that address sea level rise and ice melt for large areas. These studies primarily use input data from global and regional climate modelling efforts with spatial resolutions coarser than 10 km (see e.g. Clarke et al., 2015; Zekollari et al., 2019; Compagno et al., 2021b, a; Aguayo et al., 2024). Such climate models often have large biases when considering specific regions, which must be accounted for to represent locally accurate climate conditions where a glacier is situated. Another approach is to model single glaciers or ice caps using domain-specific high-resolution climate products. Such climate data are often limited to a few model runs (Eidhammer et al., 2021; Schmidt et al., 2020; Åkesson et al., 2025) which arguably undersample uncertainty arising from model spread. Some regions do have downscaled climate ensembles, allowing for high-resolution climate forcing with a realistic spread (see e.g. Jouvét and Huss, 2019), but this is not the case for most regions worldwide.

Recently, finely resolved convection-permitting models (CPMs) have emerged and have been shown to improve the simulated precipitation and representation of other complex topography features in comparison to regional climate models (RCMs)



of coarser resolutions (e.g. Fosser et al., 2015; Lind et al., 2020; Médus et al., 2022). These advancements are expected to
55 reduce overall uncertainty in climate projections (Lucas-Picher et al., 2021) and may improve glaciological projections and
adaptation planning in mountain communities, particularly when paired with complex SMB models. CPMs are, however, com-
putationally demanding to run. Therefore, such efforts provide model data that is limited in number of boundary forcing and
also in time periods. How the glaciological community can benefit from these new developments remains a challenge as glacier
projections require transient climate data and a representation of likely climate futures.

60 In this study, we present an approach that combines the breadth of an ensemble of relatively coarsely-resolved RCMs with
the level of detail of a CPM that covers only a few decades of the current century. This case study centres on the Folgefonna
ice cap complex in western Norway. Our research is focused on improving SMB estimates by utilizing both highly resolved
climate models and a wide range of possible climate futures. The contribution of this study is twofold:

1. We present a new framework to represent RCMs by analogs found in a spatially higher resolved dataset. This allows us
65 to include small-scale climate processes important to mountain-valley systems while evaluating a wide range of climate
model futures. In this way, we combine the benefits from climate model ensembles and detailed small-scale climate
modelling, thereby unifying the range and resolution needed for glacier projections.
2. Using this framework and the SMB model BESSI (Born et al., 2019), we provide detailed SMB simulations of the
70 Folgefonna ice cap on a 100 m spatial resolution until 2100 for three emission scenarios (RCP2.6, 4.5 and 8.5) and 117
climate model runs.



2 Data and methods

2.1 Folgefonna and the state of Norwegian glaciers

This case study centres on the Folgefonna in western Norway at around 60°N (see Fig. 1a). Although commonly referred to as a single ice cap, it consists of three plateau glaciers: Nordfonna, Midtfonna and Sørfonna. These translate to North, Middle and South fonna, respectively, where "fonna" in Norwegian means a heap of snow. Sørfonna, the largest of the three, is also the third largest ice cap in Norway, following Jostedalbreen and Svartisen. In 2018 (our most recent dataset), the highest elevation on Sørfonna was around 1650 m a.s.l. and the lowest at around 460 m a.s.l. while its thickest ice was around 540 m (Ekblom Johansson et al., 2022).

Folgefonna is situated within the Hardanger region, and experiences a maritime climate with both high rates of snowfall in winter and melt in summer. Southern Norway has a distinct separation between a coastal climate in the west and an inland climate in the east. Air masses of high humidity are carried eastward and encounter steep terrain which leads to high precipitation rates in western Norway (Konstali and Sorteberg, 2022). Previous research suggests that the mass budget of maritime glaciers in western Norway is mainly controlled by the winter mass balance (Andreassen et al., 2005; Nesje, 2023) which depends strongly on the North Atlantic oscillation index. One weather station is present on the ice cap itself, on Nordfonna at 1212 m a.s.l. For 2015–2024, the average summer (JJA) temperature was 7.3°C, while the average winter (DJF) temperature was -4.8°C (extracted from <https://seklima.met.no/>).

Downstream from Folgefonna, numerous communities depend on glacier runoff for agriculture, hydropower, drinking water, and tourism. Until recently a summer ski centre operated on Nordfonna, but it has now closed, partly due to the ice retreating too far. These local actors may all benefit from trustworthy glacier projections, but such knowledge is sparse on a highly resolved spatial scale. Scandinavian glaciers are expected to shrink substantially as a consequence of climate change. Hock et al. (2019) suggest that mass losses will vary from ~60% (RCP2.6) to ~80% (RCP8.5) by 2100 compared to 2015, while Compagno et al. (2021b) find a more pessimistic estimate of 67±18% (RCP2.6) to 90±7% (RCP8.5) by 2100 compared to 2018. A few published studies have focused specifically on Folgefonna. Ekblom Johansson et al. (2022) use a PDD model based on weather data from a station in Bergen (65 km west of Folgefonna) with a simple scaling of temperature and precipitation to represent RCP2.6 and RCP8.5. They expect Sørfonna to disappear completely for the high-emission scenario by 2170. Furthermore, Nesje (2023) estimates that Blomstølskardsbreen (Fig. 1b) will lose around 85 m w.e. in 2100 under RCP8.5 relative to 2001. In summary, we have an understanding of how severely climate change will affect Scandinavian glaciers, but no detailed spatial projections to inform e.g. adaptation policies.

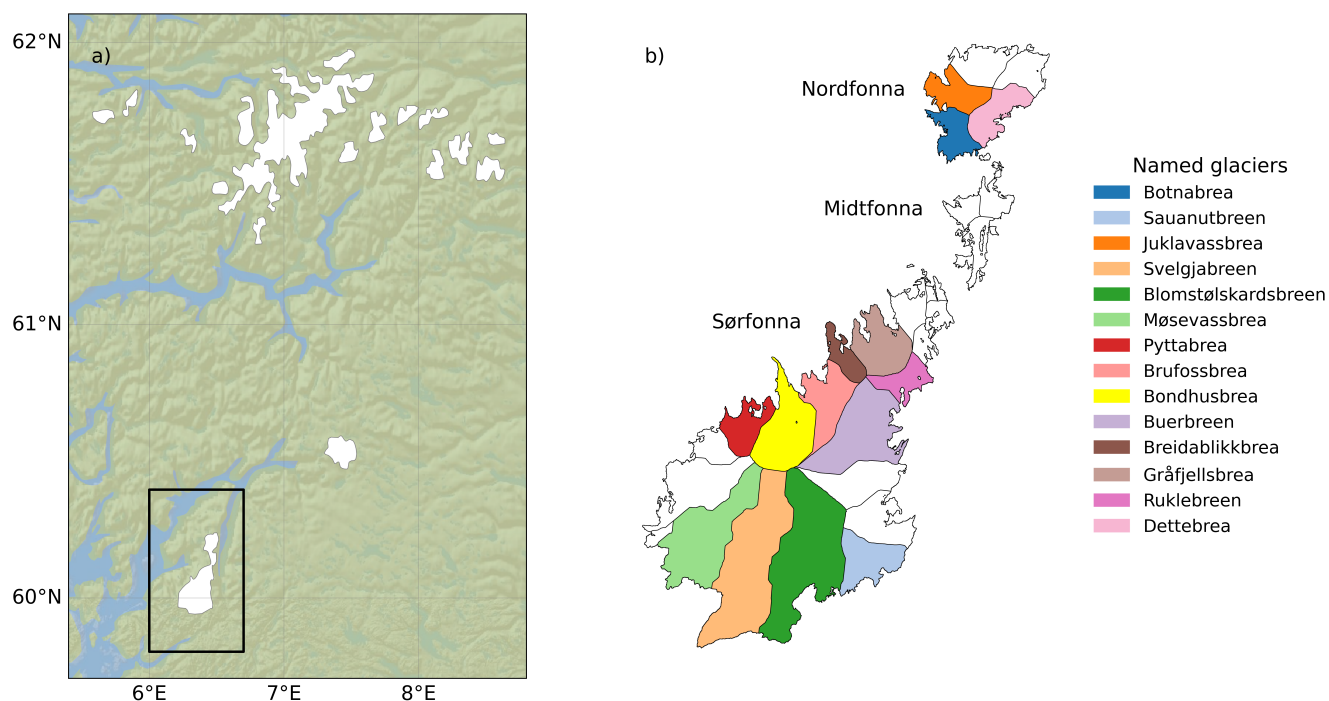


Figure 1. a) Map of western Norway where glaciers are marked in white. The region simulated with BESSI is marked with a black square containing Folgefonna, while the entire domain was used for the analog search described in Section 2.4. Map data are provided by Esri, TomTom, FAO, NOAA, USGS. In b) an overview of named outlet glaciers on Folgefonna is displayed. "Breen" and "brea" are Norwegian words meaning "the glacier". Glacier masks are provided by NVE, Kartverket, Geovekst og kommuner, Geodata AS.

2.2 SMB model setup

100 To simulate future SMB of Folgefonna, we utilize the snowpack and energy balance model BESSI, the BErgen Snow SIMulator (Born et al., 2019). It accounts for physical principles while achieving computational efficiency, allowing us to run it for a range of climate scenarios at high spatial resolution, with reasonable computational costs. The model calculates daily energy and mass balance on a three-dimensional grid (latitude, longitude and firm layers). As its climate forcing, BESSI requires temperature, precipitation, humidity, long-, and shortwave radiation. The model takes into account firm densification, heat
 105 conduction, percolation and refreezing of water, as well as snow aging and its effect on albedo. Thus, when we refer to SMB, we also include internal processes in the near-surface firm. For full model description and explanation of the model architecture, we refer readers to Born et al. (2019) and Zolles and Born (2021).

2.3 Climate forcing

Robust SMB projections require both the width of multi-model climate futures and the credibility of region-specific climate
 110 data which resolve small-scale climate effects. To achieve this we combined various sources of climate data. A convection-



permitting model, NorCP (Lind et al., 2020), has been run for the Folgefonna area at a high spatial resolution, but the runs are not transient nor do they cover the amount of likely climate futures presented by different ensembles. The EURO-CORDEX ensemble (Jacob et al., 2014) provides such a range, but has e.g. unrealistic precipitation patterns for western Norway. Consequently, interpolating ensemble member data to the Folgefonna region would likely give unphysical data. Therefore, we developed an *analog downscaling* method to bridge range and resolution. For each day of a coarse transient simulation, the algorithm selects the most similar day from another high-resolution dataset to represent it. This analog day may then also provide variables that were not available in the original transient simulation. In the following, we first introduce the three climate datasets that are used for this work. These are NorCP (high *resolution* climate data), EURO-CORDEX ensemble (representing a *range* of climate futures), and SeNorge (observational data providing *realistic* historical climate data; Lussana et al., 2018b). After introducing each climate model, we outline the analog downscaling methodology in Section 2.4, how it employs the three datasets, and validation of the method. An overview of the entire processing of climate data can be found in Figure 2.

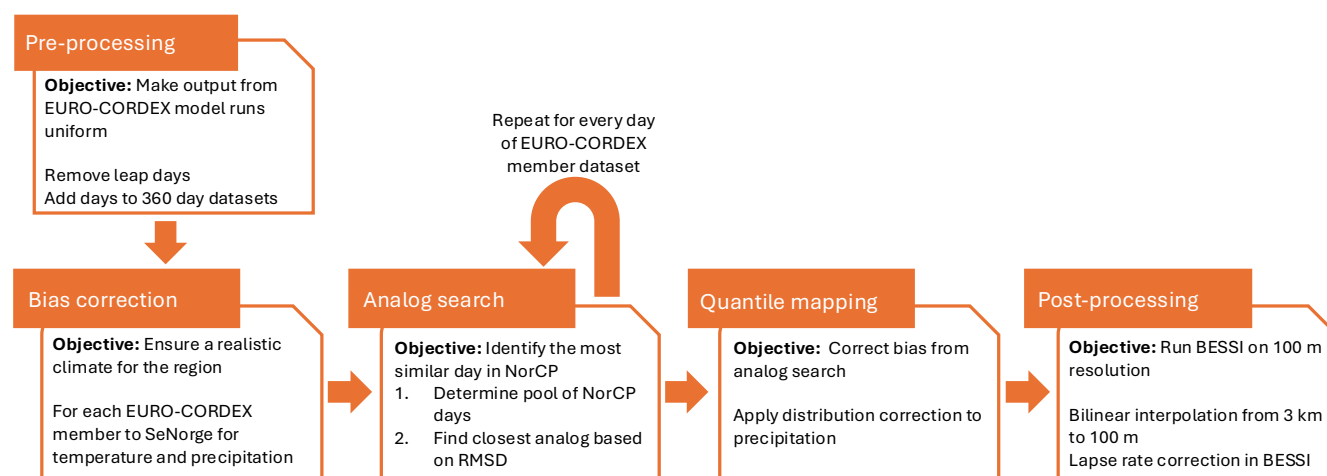


Figure 2. Schematic of the entire workflow for processing climate data.

2.3.1 High resolution: NorCP

NorCP is a convection-permitting climate model with a high spatial resolution (3 km) provided for Fenno-Scandinavia (Lind et al., 2020, 2023). It uses the HARMONIE-Climate model and is forced by dynamically downscaled GCMs EC-EARTH and GFDL-CM3. It is run for two emission scenarios (RCP4.5 and 8.5) for three 20 year periods (1985–2005, 2041–2060, and 2081–2100). The dataset also contains one historical run forced by the reanalysis dataset ERA-INTERIM for 1998–2018. This amounts to nine runs that are outlined in Table 1. To our knowledge, this dataset provides state-of-the-art simulations of climate for the Folgefonna region. However, the temporal gaps in data makes it impossible to apply directly to our SMB model since a transient climate is essential to model the snowpack and accurately project glacier changes.



Table 1. Overview of NorCP model runs.

Time period	Boundary forcing	Climate scenario
1985–2005	GFDL-CM3/EC-EARTH	Historical
1998–2018	ERA-INTERIM	Historical
2040–2060	EC-EARTH	RCP4.5/RCP8.5
2080–2100	EC-EARTH	RCP4.5/RCP8.5
2040–2060	GFDL-CM3	RCP8.5
2080–2100	GFDL-CM3	RCP8.5

130 2.3.2 Wide range: EURO-CORDEX

The EURO-CORDEX initiative (Jacob et al., 2014, 2020; Kotlarski et al., 2014) provides a wide range of RCM simulations over Europe until 2100. The ensemble has a spatial resolution of 0.11° (~ 12.5 km) and numerous combinations of GCMs (7) and RCMs (11). The three emission scenarios RCP2.6, 4.5, and 8.5 are represented each by 30, 25, and 68 model runs, respectively. For this work, we have used a total of 117 runs, with a few excluded due to missing historical data (see Appendix
 135 A). The climate models are all continuous and cover the period from 1971 until 2100. A few exceptions have their last full year in 2098 or 2099.

Across Europe, EURO-CORDEX simulations tend to be wetter and colder than both observations and reanalyses (Vautard et al., 2021). Our analysis of the western Norway area echoes this. For the entire domain in Fig. 1a, we compared median precipitation and temperature over the 1971–2005 period of each EURO-CORDEX model to SeNorge. Most models are colder
 140 (Fig. 3a) and all models are wetter (Fig. 3b) than SeNorge. The data will consequently lead to an unreasonably high SMB. Furthermore, we see that model runs with the same RCM display similar patterns. Investigations into spatial distribution found that several models (especially HIRHAM, REMO, and RCA) exhibit spurious hot spots for precipitation (up to 35 mm/day daily average) close to steep topographic changes. These models tend to have lower precipitation values at high altitudes, concealing the spatial trends when considering total precipitation for the grid.

When using the dataset in the analog downscaling method, a realistic climate is ensured by bias correcting each model run with daily climatologies for temperature and precipitation from the SeNorge model run for 1971–2005. For each EURO-CORDEX model run, we estimate the average precipitation and temperature for each grid cell for every day of the year. The resulting difference between the modelled and interpolated dataset is used to correct temperature by simply adding the daily bias. We scale the modelled precipitation by the fraction between the interpolated and modelled values. The fraction is
 150 furthermore constrained to be between 0.1 and 10 to avoid unrealistic values. Both bias corrections assume stationarity of the correction function – that is, the same bias persists into the future. We make this necessary simplification since accounting for time dependent biases is outside the scope of this work. However, note that there is evidence that biases are non-stationary especially in glacial regions due to their changing albedo under climate change (Maraun, 2012).

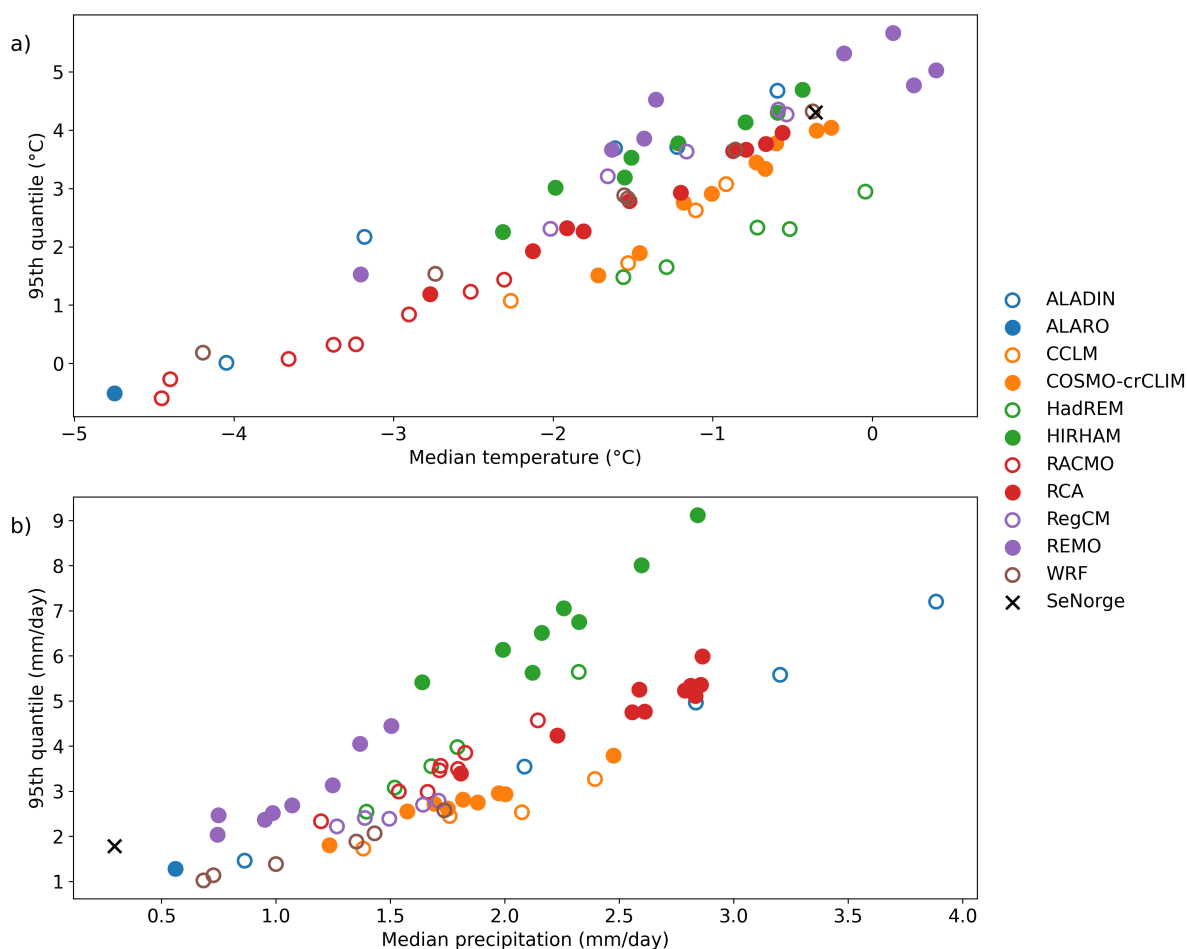


Figure 3. Median and maximum values (95th quantiles) of a) temperature and b) precipitation for EURO-CORDEX ensemble members in the past (1971–2005). Observational data (SeNorge) is marked by a black cross.

155 Although the EURO-CORDEX ensemble’s spatial resolution is excellent for a range of purposes, it is clear that it still falls short in resolving complex topography. Small-scale processes such as mountain-valley circulations, atmospheric convection and cloud physics are typically parameterised by the RCMs (Pontoppidan et al., 2017) and not resolved as well as by NorCP.



2.3.3 Accurate representation: SeNorge

SeNorge (Lussana et al., 2018b) is a very highly resolved (1 km) gridded climatological dataset over Norway spanning from 1957 to present day. It contains spatially interpolated data of temperature and precipitation based on observations from weather stations. The dataset presents state-of-the-art past climatological conditions in Norway – and Folgefonna by extension. It therefore provides us with past data that we can utilize to bias correct EURO-CORDEX data and calibrate BESSI parameters to achieve a highest possible accuracy.

Lussana et al. (2018a) find that SeNorge sometimes underestimates precipitation in data-sparse areas, such as mountainous regions. However, they also show that Hardanger, where Folgefonna is situated, is well represented by SeNorge. Though there is only one weather station on the ice cap itself (on Nordfonna), there are several at sea level by the fjord and SeNorge has been shown to represent precipitation well in station dense regions (Lussana et al., 2019). Thus, though a high mountain region, the dataset does not have the same data scarcity issues for Folgefonna as other similar areas in Norway. Obviously, an observation-based dataset lacks future data. In addition, BESSI requires radiation and humidity which makes SeNorge impossible to use directly as climate forcing.

2.4 Analog downscaling method

A possible way of representing different climate models by a high resolution RCM would be to calculate the offset between one NorCP run and each EURO-CORDEX run for all variables. For each run, a dedicated bias correction would be applied to NorCP. However, we believe that this conserves the climate variability of the high-resolution dataset, and therefore does not properly represent the coarse resolution one. Studies where climate variability is not dealt with, but rather removed by averaging, likely underestimate the impacts of climate change (Thornton et al., 2014). Climate variability is important for glacier length fluctuations and mass balance (Reichert et al., 2002; Malone et al., 2019; Zolles and Born, 2024), with a more pronounced effect when daily, rather than monthly, fluctuations are included (Farinotti, 2013). Frequency of extreme precipitation or dry periods may differ between models, and may also vary in time for the various climate scenarios. We therefore developed a framework that preserves characteristics of individual EURO-CORDEX models while resolving the local climate as NorCP would. This method can also be used for climate data which lacks required climate variables.

We represent one day in a coarse resolution climate dataset, the *target*, by finding the most similar day in a high-resolution dataset, an *analog*. This process is repeated for every day in the target dataset (each EURO-CORDEX member). The chosen analogs (chosen NorCP days) are patched together and constitute a climate dataset. From here on, an asterisk will show that we discuss a dataset that is made from analogs, i.e. modelA* is the analog downscaled dataset representing modelA. This dataset represents the target and preserves its variability and systematic biases, while also resolving the small scale climate effects provided by NorCP. A schematic of the workflow can be found in Fig. 4.

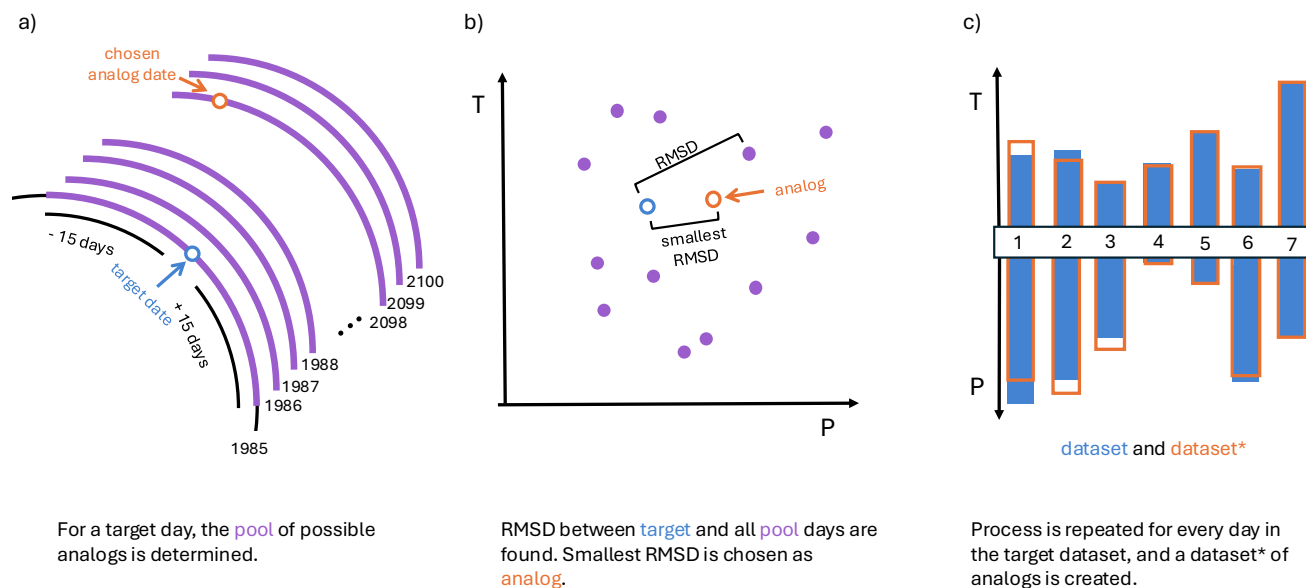


Figure 4. A visual representation of the analog downscaling process where T is temperature and P precipitation. a) The pool is determined as ± 15 days from the date of the target day, in all simulation runs and years within the high-resolution dataset. b) The day closest resembling the target is determined based upon the smallest $RMSD_{pool}$. c) All chosen analogs are patched together as a dataset* representing the original target.

The algorithm bases its choice on the patterns of only precipitation and temperature. We justify this as these variables are the most important climate forcing for SMB, and that it makes the algorithm more computationally efficient. However, the framework can easily be modified to include more climate variables. Note that the method does not account for any interdependency among climate variables.

For every day in the target data, we determine a pool of possible analogs that could represent this day. The pool is constrained to be ± 15 days from the target day in question to ensure realistic downwelling shortwave and longwave radiation values. At $\sim 60^\circ\text{N}$ (where Folgefonna is situated), there are 19 hours of daylight in the summer and less than 6 hours at the peak of winter. Downwelling radiation may therefore be dominated by shortwave radiation in summer and longwave radiation in winter. Selecting a constrained pool thus ensures that a short winter day does not represent a long summer day, even if they have similar temperature and precipitation patterns. This means that when searching for an analog for the 15th of May, the pool of possible analogs ranges from 1st of May to 30th of May for all simulation years and runs contained in NorCP (see Table 1). We suggest that the criterion (± 15 days) is reevaluated for regions at other latitudes. The pool of possible analogs always consists of 5580 days due to the ± 15 day criterion and 20 years in each of the 9 NorCP runs ($31 \cdot 20 \cdot 9 = 5580$).

Each day in the pool of possible analogs is then compared to the target day. The root mean square deviation (RMSD) of the two-dimensional precipitation and temperature fields of the target day is calculated compared to all pool data. This is performed over the western Norway grid shown in Fig.1a. The RMSDs are normalised by dividing by the mean of all values in the pool.



Then, the normalised RMSDs for temperature and precipitation are summed, creating a single measurement of how close each possible analog is to the target day. Since the climate data are on a two-dimensional grid, the summation of squared differences is done for every grid cell i . For each day in the pool, $RMSD_{pool}$ is thus estimated by

$$RMSD_{pool} = \sqrt{\frac{\sum_{i=0}^N (t_{i,target} - t_{i,pool})^2}{N}} \cdot \frac{1}{\bar{t}_{pool}} + \sqrt{\frac{\sum_{i=0}^N (p_{n,target} - p_{i,pool})^2}{N}} \cdot \frac{1}{\bar{p}_{pool}}, \quad (1)$$

where N is total amount of grid cells, and t and p are temperature and precipitation, respectively. After estimating $RMSD_{pool}$ for each day in the pool, the day with the smallest value is considered to be the one closest resembling the target day and is therefore chosen as an analog for the target day (see Fig. 4b). The method is repeated for all days in the target dataset, and the analogs (chosen NorCP days) are patched together in their original high spatial resolution representing the target (a EURO-CORDEX run). As an example, we show how the temperature of one target day is represented by its analog (Fig. 5).

The algorithm requires the two datasets to be on the same grid to compute the difference between the same grid boxes (Fig. 5). The higher resolution dataset (Fig. 5c) is therefore interpolated (nearest neighbour) to the grid of the lower resolution dataset (Fig. 5b), since this is more computationally efficient than the other way around. For EURO-CORDEX*, we work with the entire domain in Fig. 1a, while for SeNorge*, we use the square domain around Folgefonna.

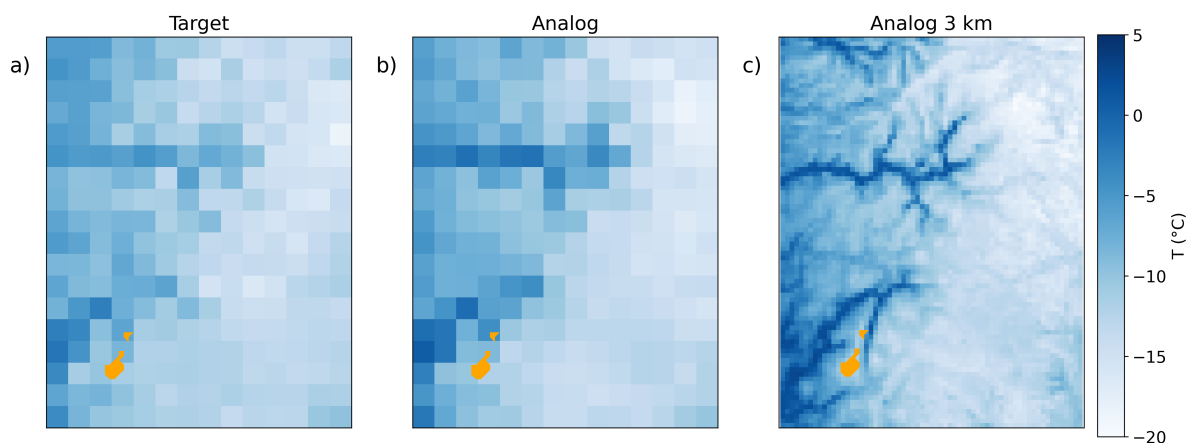


Figure 5. Example of how the bias corrected 3-Jan-2006 in the EURO-CORDEX run ICHEC-EC-EARTH-r1i1p1-RACMO22E-v1 (a) is represented by 29-Dec-1987 from the NorCP GFDL-CM3 dataset (b), as well as the same field on NorCP’s original resolution of 3 km (c). An outline of Folgefonna is marked in orange on all three maps.



Validation

To validate that the analog downscaling method can mimic a realistic climate, we investigate whether it leads to any systematic biases. For this purpose, we use the analog downscaling with the NorCP ERA-INTERIM (NorCP-ERAi) run over 1998–2018 as target. The algorithm was constrained to not choose itself to avoid a duplicate dataset, but was otherwise kept the same.

220 Systematic biases are investigated by looking at the median differences in precipitation and temperature between the analogs, NorCP-ERAi*, and target, NorCP-ERAi, for each season. We find no noticeable bias in temperature (Fig. 6d), but a slight underestimation of precipitation (Fig. 6b). Independently of precipitation amount, the analogs have 3-7% less precipitation than the target. This amounts to a median difference of less than 0.15 mm/day. We attribute the underestimation to the shape of the precipitation distribution (Fig. 6a). It has most events at no and low precipitation, and quickly tapers off for higher
225 values. Consequentially, for any given target, there are more suitable analogs that underestimate, rather than overestimate, precipitation. The underestimation is corrected for by applying quantile mapping to NorCP-ERAi*. This is done by finding the cumulative distributions of precipitation in NorCP-ERAi* and NorCP-ERAi. The differences between quantiles in the datasets are found and added to NorCP-ERAi*. Since the pool always consists of NorCP data and the precipitation distribution is constant, we use the same quantile mapping-distribution independently of target dataset. The correction reduces the bias to
230 2.7% in the summer months (JJA) and an overestimation of 1.8% in the winter months (DJF).

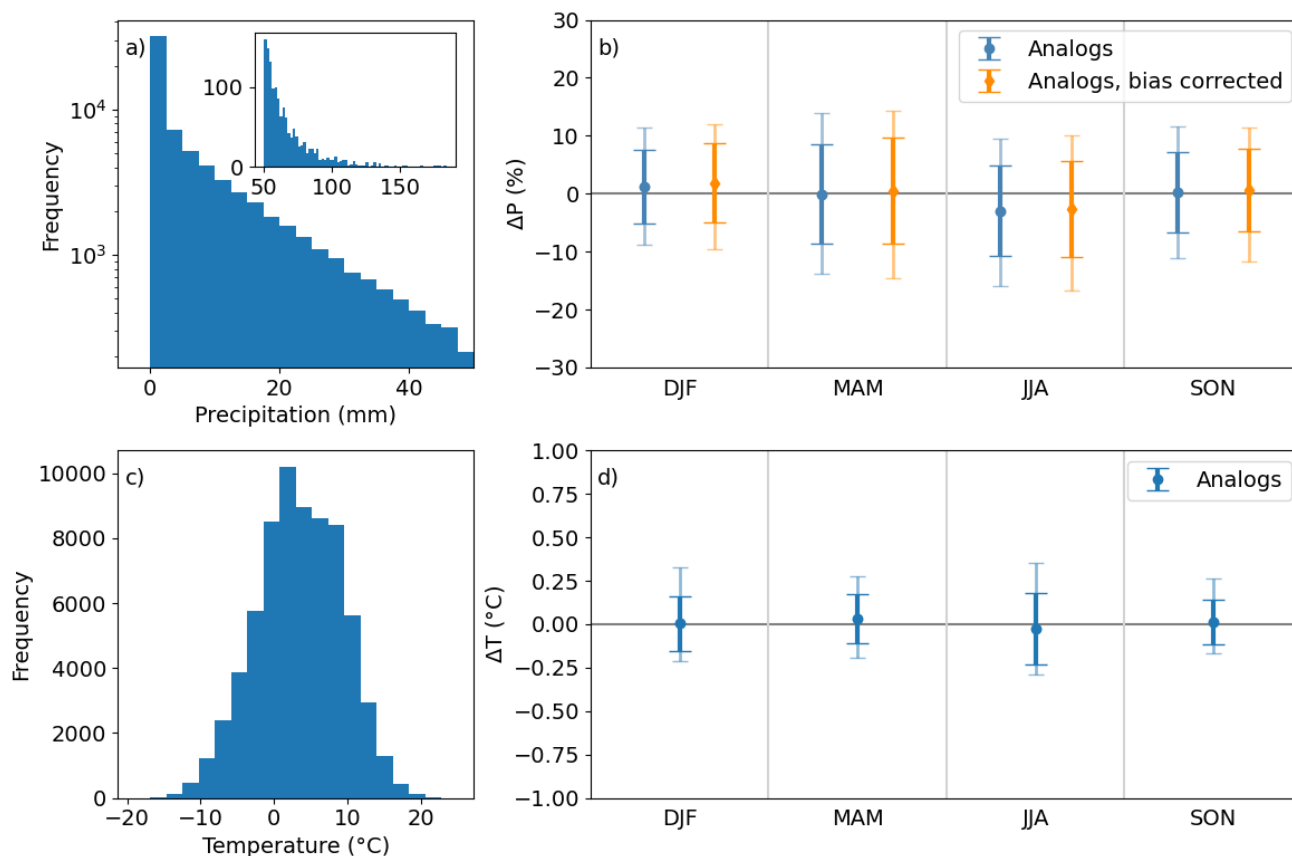


Figure 6. Upper panel shows a) the distribution of spatially averaged precipitation in the pool data, and b) in blue is the median difference in precipitation between target and analogs for each grid point, averaged over a season. Darker whiskers show the standard deviation and the lighter show 5th and 95th quantiles. Orange shows the same for the bias corrected data. The lower panel shows similarly the c) distribution and d) median difference for temperature. Here, no bias correction has been performed.

2.5 Calibration

BESSI's parameters have previously been calibrated to climatic conditions of the Greenland ice sheet (Born et al., 2019; Zolles and Born, 2021). In a milder western Norway climate, we expect parameters in the SMB model (such as snow albedo) to change. We therefore ran BESSI with a range of parameters for 1960–2020 using SeNorge*. The parameters chosen for calibration were sensible heat flux, as well as albedo of fresh snow, wet snow, and bare ice. In total, 100 different parameter sets were tested whose combinations were determined by latin hypercube sampling (McKay et al., 2000) which samples randomly within parameter ranges while covering the full parameter space using the framework provided by Perrette (2013). The parameters, ranges and chosen best parameter set are shown in Table 2.



Table 2. Parameters calibrated in past simulation runs. The tested range and found optimal value are also depicted.

Parameter	minimum	maximum	chosen value
Fresh snow albedo	0.65	0.9	0.85
Firn albedo	0.45	0.7	0.56
Ice albedo	0.3	0.4	0.33
Sensible heat flux ($\text{Wm}^{-2}\text{K}^{-1}$)	5	25	8.95

Each of the calibration ensemble members were evaluated by how well they could reproduce historical mass balance provided by the Norwegian Water and Energy directorate (NVE). Outlet glaciers on Folgefonna have been monitored in two periods between 1963–1981 and 2003–2017. Midtfonna, Ruklebreen, and Bondhusbrea only have measurements for the early period, while Blomstølskardbreen and Møsevassbrea only have measurements from the latter. Gråfjellsbrea, Breidablikkbrea, and Svelgjabreen have measurements from both periods (see Fig. 1b for basin overview). To use a range of calibration criteria, we compared the 100 runs both to basin estimates and single stake measurements (obtained by pers. comm. with B. Kjöllmoen, NVE). The stakes are solely on Sørfonna, but are well distributed along both north-south and west-east gradients (Fig. 7b). Hence, we approached the calibration in two different ways:

1. Calculating the SMB for the basins: The cumulative SMB over the measurement period is estimated for each grid point within the basin and averaged.
2. Calculating the SMB for each stake: The cumulative SMB over the measurement period for each stake is estimated for the corresponding grid point in BESSI. Onset of accumulation and ablation seasons vary in the dataset, and we use the same dates to estimate SMB in BESSI for each stake measurement. Measurements that are missing the start date of accumulation season are discarded and not used in the calibration.

Working with several criteria can illuminate which parameter sets perform best for different conditions. We therefore tested a few, which are RMSD, mean absolute error (MAE) and Nash-Sutcliffe efficiency (NSE) (Nash and Sutcliffe, 1970; Gupta and Kling, 2011). To further create several evaluation criteria, we split the stakes into high and low elevation stakes (above/below 1300 m a.s.l.). However, only minor differences were found. Out of the four consistently best parameter sets, two of them contained extreme values for albedo parameters, while the other two had similar values well within the expected ranges. Therefore, we chose one of these as our final tuning of the parameters as shown in Table 2. The modelled SMB values are plotted against the observed in Fig. 7a along with the identity line. We found that the performance of the different runs is highly dependent on the sensible heat flux. None of the quality measurements (RMSD, MAE, and NSE) showed any apparent dependence on the three albedo parameters (albedo of fresh snow, firn, and ice). We hypothesize that this could be due to the cloudy climate in western Norway and recommend recalibration for new regions. The average RMSD for the 10 best runs is 88 cm w.e. (stakes) and 61 cm w.e. (basins), indicating that we can expect an error in our SMB model of ± 0.88 m.w.e..

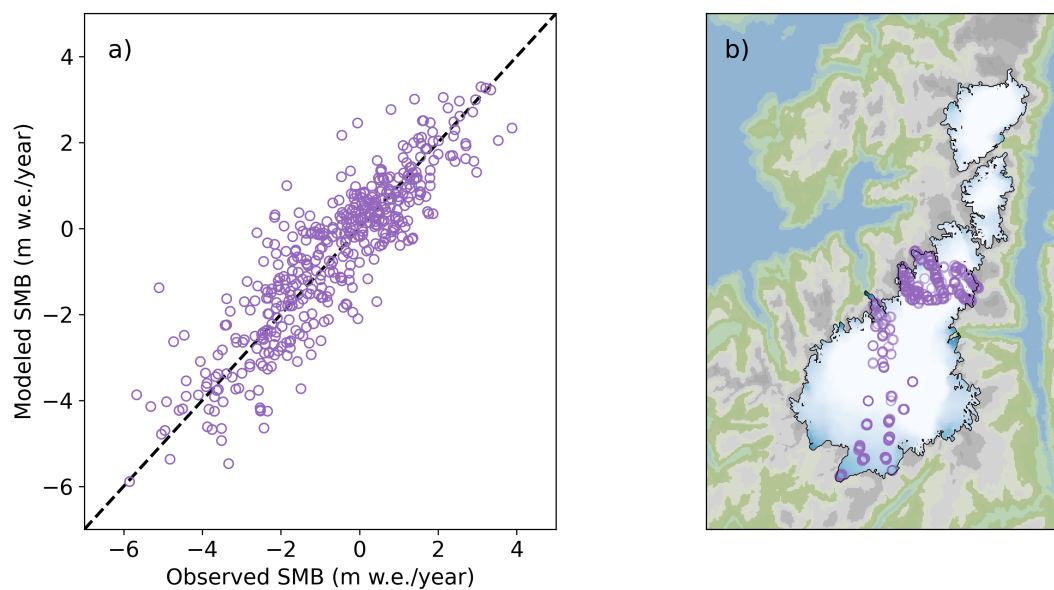


Figure 7. In a) the modelled SMB using calibrated parameters (Table 2) is plotted against the observed SMB along with a dashed identity line ($x = y$). In b) the location of stake measurements are indicated.



265 3 Results

We integrate the SMB over the entire Sørfonna plateau and look at the median of models along with the spread (represented by 25th and 75th quantiles) of each scenario for every year. The probability of Folgefonna occasionally experiencing years with positive mass balance decreases quickly and it becomes highly unlikely after 2050 for all scenarios (Fig. 8a). Until 2060, the three emission scenarios are indistinguishable within their uncertainty. From 2060–2100, the bounds of RCP2.6 and RCP4.5 generally overlap, while RCP8.5 shows a much more severe response to climate change. Similarly, the temperature in the three emission scenarios start to diverge mid-century (Fig. 8c). Median net SMB is ~ 0.9 m w.e./year for 1970–2000. Averaged over 2090–2100, the median annual net SMB decreases to -0.4 ± 0.8 , -0.9 ± 0.9 , and -3.1 ± 1.0 m w.e./year for the low, middle, and high emission scenarios, respectively.

The cumulative SMB shows how mass loss will compound until the end of the century (Fig. 8b). When looking at the median cumulative SMB among model runs, we find that for the most optimistic scenario, the entire ice cap will experience around -15 m w.e. of mass loss until 2100 from today (2025). For RCP4.5, the cumulative SMB decreases to -50 m w.e. and for RCP8.5, it reaches around -105 m w.e. As the mass loss compounds, so does its spread due to climate models. At the end of the century, RCP2.6, 4.5, and 8.5 have spreads of 65, 67, and 75 m w.e., respectively. For the calculation of net and cumulative SMB, we used a static glacier mask for Sørfonna. We exclude Nordfonna and Midttonna as we expect them to have larger relative area changes over the century as they are smaller from the onset.

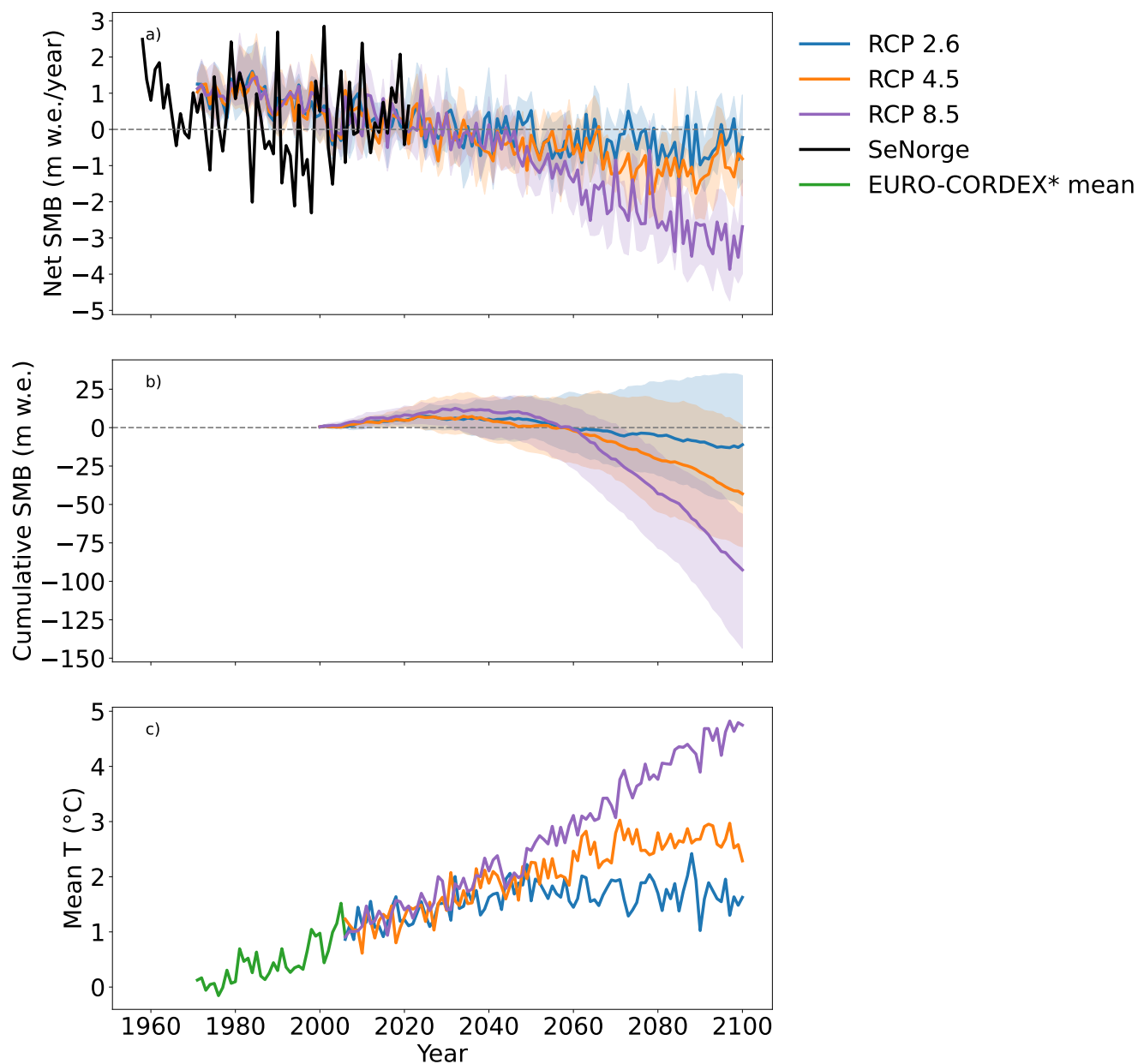


Figure 8. In a) the ensemble median of spatially averaged SMB for Sørnfonna is plotted per simulation year. Medians of RCP2.6, 4.5 and 8.5 are shown by solid lines, while shaded areas indicate their 25th and 75th quantiles. The same is plotted in b), but for median cumulative SMB over Sørnfonna from today (2025) until 2100. Finally, in c) the annual temperature for the entire western Norway domain is plotted for each scenario. The historical curve is an average of all EURO-CORDEX* models.



3.1 Inter-model differences

After having established the differences between emission scenarios, we have a closer look at inter-model differences within the scenarios. For each of the model runs in RCP8.5, we average SMB over the entire Sørfonna ice cap, similarly to Fig. 8a. In addition, we average SMB over the last simulated decade (2090–2100) for every BESSI model run with the EURO-CORDEX* ensemble. We sort the models after which GCM and RCM they are forced by (Fig. 9). We see that the spread between models belonging to the same GCM groups are smaller than between the models forced by the same RCM. When looking at the GCM groups, model runs based on HadGem2-ES result in the most negative SMB, while those based in MPI-ESM yield the most positive (Fig. 9b). For every RCM group, HadGem2-ES also gives the most negative SMB, and MPI-ESM the highest (Fig. 9a), despite there being overlap with other GCM groups (Fig. 9b). We found similar tendencies for the same GCMs in the smaller sub-ensembles RCP2.6 and RCP4.5 (Appendix B).

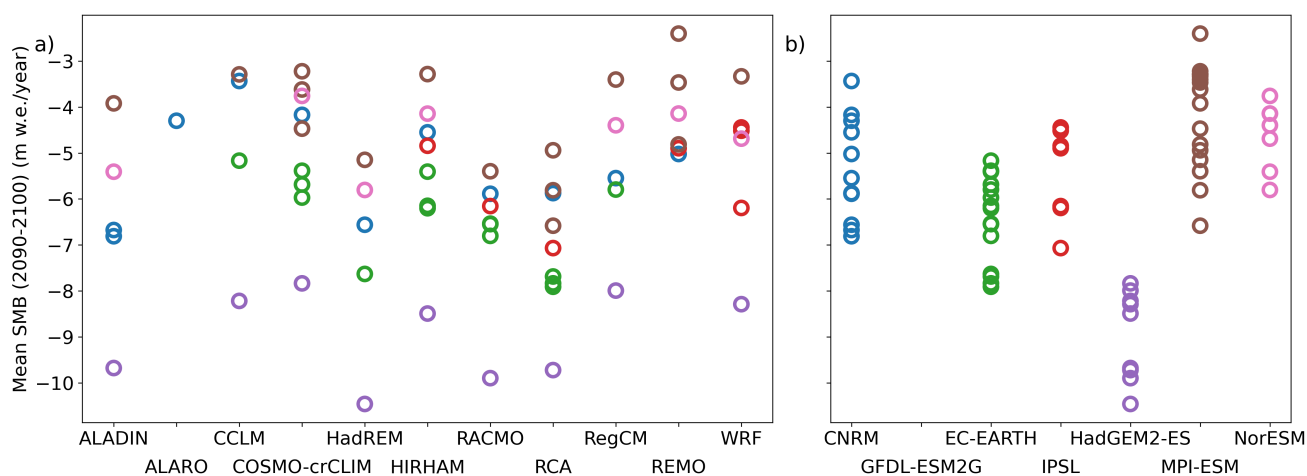


Figure 9. Spatially (over Sørfonna) and temporally (over 2090–2100) averaged SMB for each BESSI model run in the EURO-CORDEX* RCP8.5 scenario. Mean SMB is sorted after which a) RCM, and b) GCM the climate data stems from. The data is colour coded by which GCM they belong to in both plots. Data with same RCM and GCM differ from different ensembles or RCM version (Aladin53_v1/Aladin63_v2 and REMO2009_v1/REMO2015_v1).

3.2 Spatial changes

We consider how the SMB is distributed over the ice cap as an average of 25–30 year time periods (Fig. 10). By the end of the century, there are accumulation zones on both Sørfonna and Nordfonna for RCP2.6. For RCP4.5, there is only one on Sørfonna, and for RCP8.5 all accumulation zones have disappeared by 2100. A model median seems to represent past climatic response of the SMB well. For 1970–2000 it overestimates SMB on the Northern part of Sørfonna, while for 2001–2025 it reaches a similar equilibrium line altitude (ELA) as the one resulting from the SeNorge* run. Note that in the historical runs, the emission scenarios differ because they contain different sets of EURO-CORDEX* models.

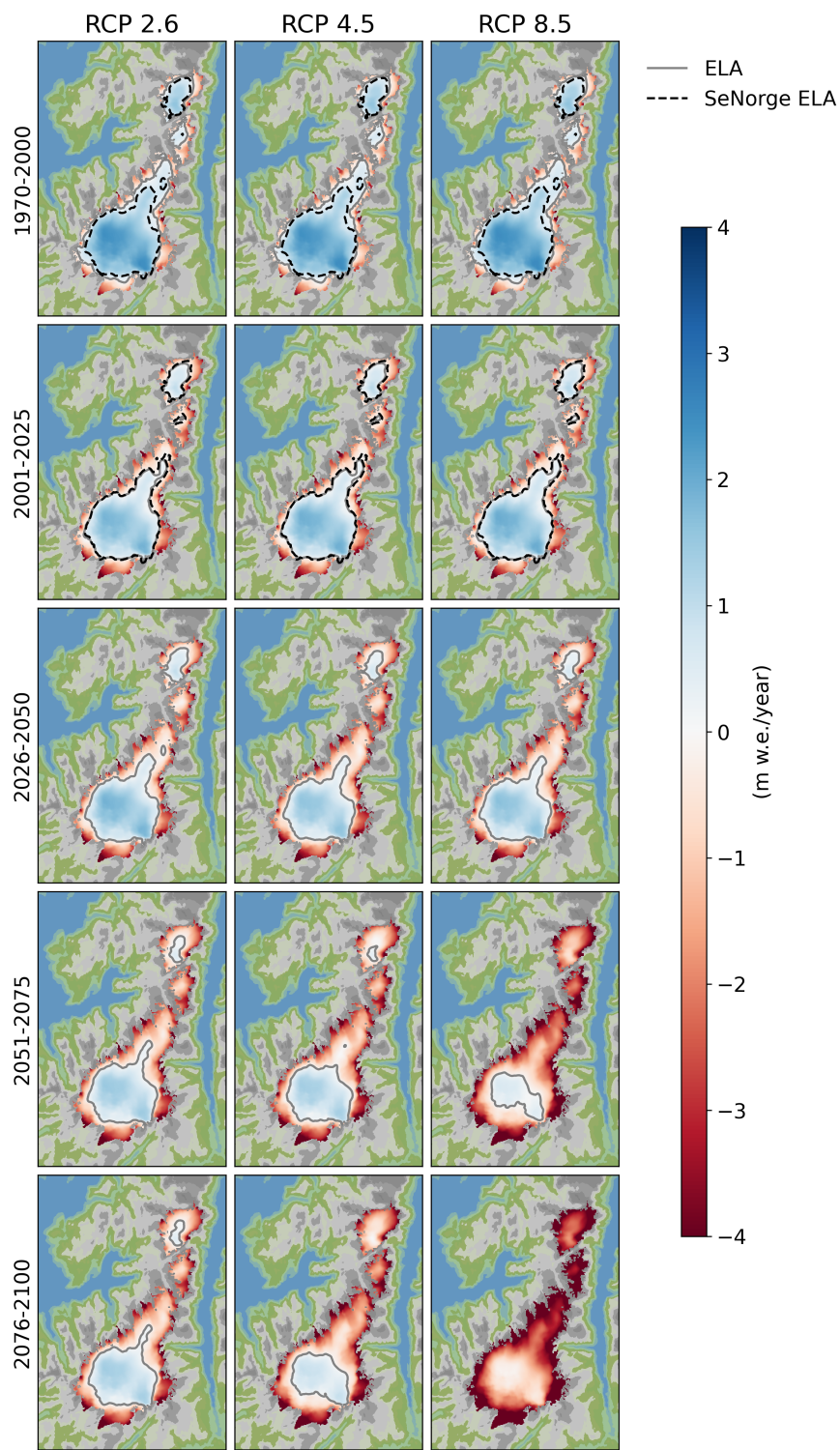


Figure 10. Median SMB of all models in 25-30 year periods for each of the emission scenarios. ELAs for both median of the EURO-CORDEX* ensemble (solid contour) and the SeNorge* run (dashed contour) are indicated.



Furthermore, we notice that the ice cap has a more negative SMB on the eastern part, with positive SMB becoming slightly skewed towards the west. This is also visible for Midtfonna in the past. The eastern glaciers tend to have a more negative SMB that stretches further in on the ice cap, especially after 2050. To test if this indeed is the case, we conducted additional analysis. For every grid point on Sørfonna, we fitted a linear regression to SMB over time (2026–2100) to RCP8.5. Slope is plotted against elevation in Fig. 11b, where the basins are divided into groups terminating on the eastern or western side (Fig. 11a). The western area is larger and therefore contain more data points. Each of the "tails" belong to specific basins. For elevations higher than 1300 m a.s.l., the western and eastern parts are mostly overlapping. At lower elevations, however, the eastern side seems to consistently yield smaller slopes i.e. be more robust to climate change. The lower elevations are naturally also where the longitudinal distance is furthest between the western and eastern sides.

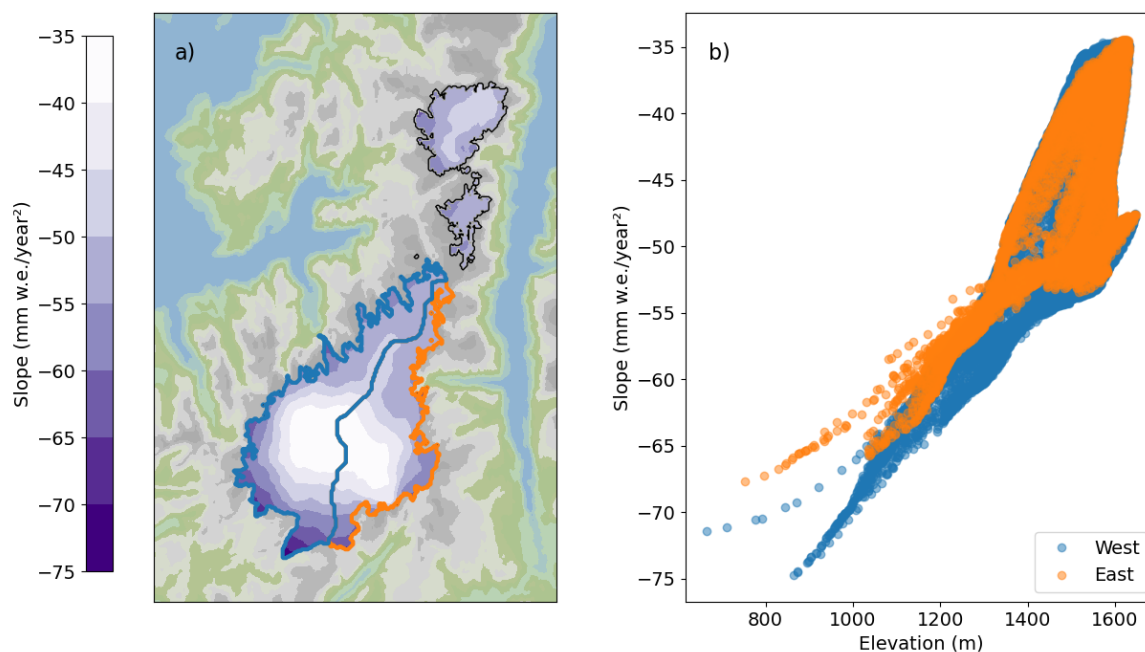


Figure 11. Slope of SMB from a linear regression of net SMB 2026–2100 for each grid box on the ice cap. In a) it is plotted after location, where main eastern and western basins are marked, while in b) the slope of each grid cell is plotted against its elevation and coloured dependent on whether it belongs to the eastern (orange) or western (blue) part of Sørfonna.



3.3 Seasonal dependence

Following up on the discussion about mass budget drivers of maritime glaciers (Section 2.1), we identify the dominant climatic controls on Folgefonna’s SMB. We evaluate correlations between total SMB and winter/summer SMB, precipitation, and temperature. The hydrological year is defined with accumulation season from October to May and ablation season between June and September. Analyses were conducted for Sørfonna as a whole, without adjusting for future lengthening of the ablation season. However, we ran experiments changing seasonality to DJF and JJA as well as only Blomstølskardsbreen. All configurations gave similar results.

We find the correlation for each climate model, and report the median with their standard deviation in Table 3. The results show a more complicated picture than what has been suggested by Andreassen et al. (2005) and Nesje (2023). Total SMB is highly correlated with both its summer and winter parts as expected (being a sum of the two). More surprising is that its correlations with seasonal temperature (averaged) and precipitation (summed) are not clear for neither the past, nor for RCP2.6 and RCP4.5. One trend that does become clear, however, is that as temperatures rise further in RCP8.5, both winter and summer temperatures are negatively correlated to the total SMB. In addition, the correlation with summer SMB is significantly larger for RCP8.5 than the other scenarios.

Table 3. Pearson correlation coefficients reported for the total yearly SMB with its summer and winter components as well as winter and summer temperature, and winter precipitation. Uncertainty is simplified to the standard deviation. Presented here are the median of all models, with the past model ensemble being the models contained in RCP8.5 (since it contains highest number of models).

SMB _{total} correlation	SMB _{winter}	T _{winter}	P _{winter}	SMB _{summer}	T _{summer}
Past (1970–2025)	0.79 ± 0.07	−0.02 ± 0.00	0.13 ± 0.13	0.72 ± 0.08	−0.12 ± 0.12
RCP2.6 (2026–2100)	0.78 ± 0.10	−0.03 ± −0.01	0.11 ± 0.13	0.72 ± 0.08	−0.05 ± 0.10
RCP4.5 (2026–2100)	0.79 ± 0.05	−0.10 ± 0.14	0.01 ± 0.10	0.77 ± 0.07	−0.17 ± 0.18
RCP8.5 (2026–2100)	0.81 ± 0.05	−0.47 ± 0.09	−0.04 ± 0.15	0.87 ± 0.05	−0.53 ± 0.15

3.4 Changes in runoff timing

As summer and winter temperatures increase, the accumulation season will shorten, while the melt period will lengthen. How will runoff patterns change in a warming climate? With no ice flow model, we cannot give estimates of total water released from the glacier. Instead, we investigate the timing of runoff resulting from melting of the snow and water that is not retained by the snowpack as well as rain that falls where the snowpack is already melted away (within one glacier basin). For each model run, and the decades 2000–2010 and 2090–2100, we integrate runoff over a glacier basin and find daily averages for the decade. We further smooth the data over 3 day periods to avoid spurious effects. Typically, any year has a melt period that starts in spring and quickly reaches its peak before it decreases throughout late summer (Fig. 12a). To find the onset of melt, we determine a threshold above which we assume runoff to be part of spring melt, and not e.g. due to spurious winter precipitation events. The first day above this threshold we define as the onset of spring melt that year. This is repeated for every model run



for one glacier basin. As an example, we show how timing of runoff changes for Møsevassbrea (see Fig. 1b) over the century for one model (Fig. 12a). We determine the threshold to be half of the average annual maximum runoff for the basin. The probability density function (PDF) of days earlier (expedited) runoff within each emission scenario is plotted in Fig. 12b. From the distribution peaks it can be seen that spring runoff is projected to occur about 6, 16 and 27 days earlier for RCP2.6, 4.5, and 8.5, respectively.

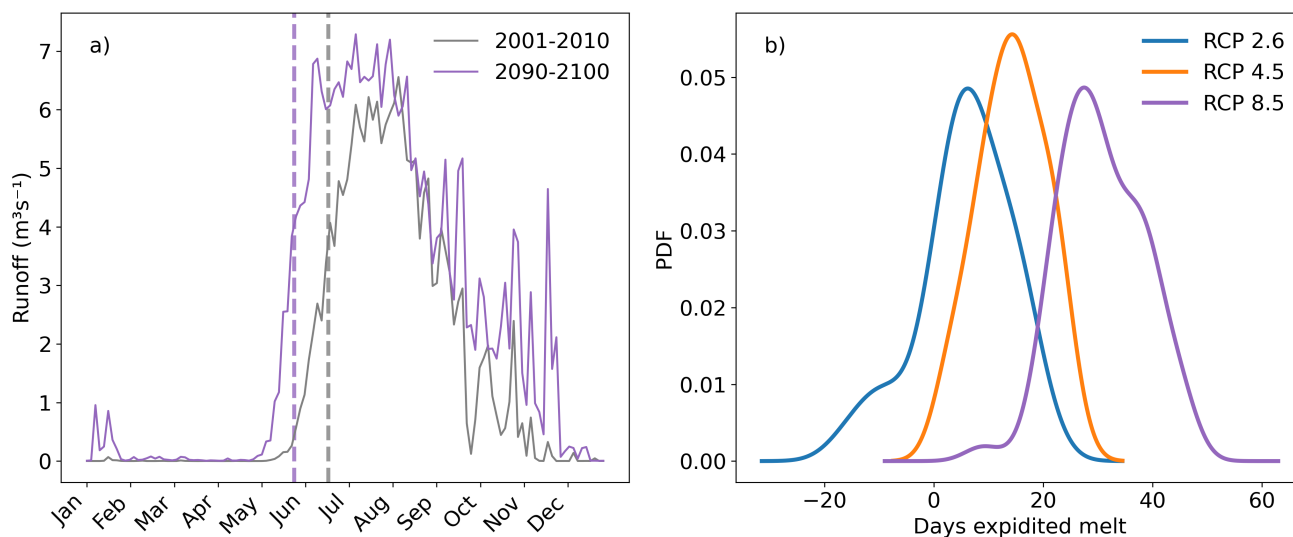


Figure 12. Changes in onset of runoff at the end of the century (2090–2100) compared to the beginning (2000–2010) for Møsevassbrea. In a) an example of the mean melt over the two decades is shown for the RCP8.5 model EC-EARTH-r1i1p1-RACMO22E-v1. Onset of melt seasons is marked by vertical lines for the two periods. In b) probability density functions of earlier runoff from models contained in each scenario are shown.



4 Discussion

4.1 Effect of emission scenario

By the end of the century, different emission scenarios have a clear impact on Folgefonna's future in terms of accumulation zone extent. Our simulations show that Midtfonna will completely lose its accumulation zone by 2050 for all emission scenarios (Fig. 10). Nordfonna loses its accumulation zone by the end of the century under RCP4.5. Since melt elevation feedback is not included in the BESSI simulations, these estimates should be regarded as conservative. Accounting for elevation changes would further increase mass loss, making it likely that even the small accumulation zone projected on Nordfonna under RCP2.6 will disappear. Whether any part of Folgefonna will have an accumulation zone beyond 2100 is contingent on warming not exceeding RCP4.5 levels. The future of Folgefonna hinges on emission scenario, in agreement with projections for glaciers worldwide (Rounce et al., 2023; Marzeion et al., 2020) and in Scandinavia (Compagno et al., 2021b).

The ice cap's total mass loss and changes in spring melt timing depend on both emission scenario and the choice of climate model. The three scenarios yield comparable net SMB until they begin to diverge around 2050 (Fig. 8a). Net SMB over the ice cap under RCP8.5 is distinct from that under the two lower emission scenarios, as indicated by the non-overlapping interquartile ranges. Meanwhile, the two lower emission scenarios remain indistinguishable within their interquartile ranges. Similarly, we see differences in earlier spring melt that depend on emission scenario (Fig. 12b). While the full distributions overlap across scenarios, the magnitude of change increases clearly with warming. Both net SMB changes (Fig. 8a) and days of earlier spring melt (Fig. 12b) approximately double from RCP2.6 to RCP4.5, and double again from RCP4.5 to RCP8.5. For the western Norway grid, the temperature anomaly compared to 1970–2000 is expected to do the same (Fig. 8c). Mean of EURO-CORDEX* temperatures (2090–2100) indicate a western Norway warming of 1.3°C, 2.3°C, and 4.3°C for respectively RCP2.6, 4.5, and 8.5. Changes in SMB and days of earlier melt therefore seem to change in step with temperature rise, and not respond nonlinearly to climate change as other studies find for the Greenland ice sheet (Mikkelsen et al., 2018; Born et al., 2019) and mountain glaciers (Bolibar et al., 2022).

4.2 Climatic drivers of SMB

The western side of Folgefonna is not more robust to climate change than the eastern. Since precipitation is mostly carried along a west-east gradient (Konstali and Sorteberg, 2022), we expected the western side of the ice cap to experience a climate change alleviation due to the increased precipitation. However, our simulations rather suggest that the eastern side is more robust to climate change (Fig. 11). The coastal-continental transition which is clear for all of Southern Norway is not detectable over spatial scales covered by the strongly maritime Folgefonna. Instead we detect an elevation-dependent difference in the ice cap's robustness to climate change (Fig. 11b), where SMB decreases faster at lower elevation. This effect is not caused by melt elevation feedback since BESSIs elevation is static in the simulations. Instead, we expect that it is due to a feature of the maritime, mild climate around Folgefonna. A small uniform temperature offset across the ice cap is more likely to increase temperatures above freezing at lower elevation than at higher elevation.



According to our simulations, total SMB becomes more dependent on temperature as warming increases, especially seen for RCP8.5. We confirm that ablation season temperature will increase its influence on SMB (Nesje et al., 2008; Giesen and Oerlemans, 2010), but add that this is also true for winter temperatures. However, our results do not support previous findings (see e.g. Andreassen et al., 2005) that the total SMB of maritime glaciers depends more on winter mass balance than on summer mass balance. We furthermore found no robust correlation between total SMB and winter precipitation. These results suggest that the processes governing annual SMB are not well captured by seasonal mean temperature or accumulated precipitation alone. This could indicate that other climatic variables, such as radiative fluxes, may play an important role in Folgefonna's SMB. Alternatively, SMB sensitivity may be dominated by short-lived events, rather than seasonal averages. For example, a few warm summer days may contribute disproportionately to melt compared to an overall warm summer.

4.3 Climate model uncertainty

These results show that accounting for ensemble spread is important for glacier projections. Each EURO-CORDEX member undergoes extensive data treatment (Fig. 4) to ensure a realistic climate for western Norway (bias correction) and to represent important high-resolution effects (analog downscaling). This processing was imperative to create a realistic climate forcing, as several EURO-CORDEX members strongly disagree with observational data (Fig. 3), and are not of a spatial resolution that can represent Folgefonna (Fig. 5a). We anticipated that this level of processing might substantially reduce inter-model differences, particularly because all final forcing fields are drawn from the NorCP dataset. Yet, we find large differences between the models (Fig. 8). This is likely due to the preserved climate variability of the climate model data. Following this, we highlight the importance of resolving ephemeral climate events for SMB estimates, consistent with previous research (Farinotti, 2013; Malone et al., 2019; Zolles and Born, 2024). Similarly to the study by Zekollari et al. (2019), we find that choice of GCM is important for SMB (Fig. 9) and that this contribution is detectable throughout the entire downscaling framework. This persistence likely reflects the role of large-scale circulation biases and differences in climate variability, which are not removed by local bias correction or high-resolution representation. These findings make it clear that projecting glacier change at a fine spatial resolution can yield results that do not carry a realistic uncertainty unless the spread in climate futures is taken into account. Highly resolved glaciological models may therefore convey a false sense of security in the absence of climate models commensurate in their ability to project highly resolved processes.

In this study, we have presented the analog downscaling method which is a novel, yet simple, approach to account for ensemble spread using detailed climate models that only contain a few runs. The method provides a pragmatic solution that enables end-users to benefit from recent advances in climate modelling, even though these models are too computationally demanding to be run continuously over a full century. This was, for example, the case for the convection-permitting model, NorCP, used in this study. The method can therefore be used to fill gaps in climate data. The analog downscaling method was developed to match analog to target based on their similarity in temperature and precipitation (Section 2.4). Restricting the match criteria to these two fields is additionally advantageous as it enables the method to be used in cases where climatic variables are missing. This was, for example, the case for the SeNorge dataset, which provides only temperature and precipitation values. In this case, analog downscaling does not strictly "downscale" the data, but produces a dataset (SeNorge*) which has all five climatic



variables as required by BESSI. While machine learning approaches can potentially address similar challenges, the analog downscaling method offers a computationally efficient and transparent alternative to benefit from climate modelling advances.

The lack of agreement between climate models remains a main caveat in providing reliable climate information for local communities. Åkesson et al. (2017) showed that Hardangerjøkulen, a relatively flat ice cap in Norway, would almost completely perish for mass imbalances of 0.2 m w.e.. Thus, changes in SMB much smaller than what is represented by the EURO-CORDEX* ensemble can be detrimental for an ice cap. Our analysis relies on standard ensemble statistical methods such as medians and quantiles, which are widely used in the community. We further find that an ensemble median reproduces historical SMB reasonably well (Fig. 10). Nevertheless, it is important to note that an ensemble median bears no real physical significance. A multimodel ensemble is a collection of representations of a physical system, rather than measurements with varying accuracy of some true value. Importantly, climate models are interdependent since they tend to have shared genealogies as the community exchanges codes and ideas (see e.g. Masson and Knutti, 2011; Knutti et al., 2013). As a result, they may neglect similar physical processes, leading to shared structural uncertainties (Qian et al., 2016). Similar tendencies are observed in ice sheet modelling (Aschwanden et al., 2021). Using a median accompanied by its quartiles is a simple way of communicating glacier projections and their uncertainties, but other approaches may be better suited. Firstly, instead of evaluating glacier projections from ensemble statistics, end-users could benefit from weighing the relevance of different climate models. This requires a well-documented hierarchy of which models perform well under certain topographical and climatic conditions. Secondly, greater agreement within regional climate models would be a key step toward more robust and trustworthy glacier projections. Both approaches hinge on the expertise, advice, and scientific advances of the climate modelling community.

4.4 Methodological limitations

Bias correction of climate data has been found to introduce additional uncertainty to projections, especially for regional scales (Weathers et al., 2025). Scaled bias correction, like we used to adjust precipitation, risks amplifying precipitation patterns out of proportions. We mitigated this risk in two main ways. First, we imposed lower and upper bounds for the precipitation scaling fraction. Second, all data that forces BESSI originate from NorCP rather than bias corrected EURO-CORDEX output. As a result, none of the downscaled EURO-CORDEX* ensemble members will have unphysical climatic patterns or values as can arise from bias adjustment methods.

The focus of this work was the effect of climate data and ensemble spread on SMB. We therefore used BESSI, a medium complexity model, to gauge the influence of EURO-CORDEX* spread. The application of BESSI to small scale studies may be improved by adding complexity such as wind redistribution and shading due to topography. Another omission from the SMB model setup is the lack of elevation feedback as the ice cap melts. This would likely increase mass loss of the ice cap and our estimates can therefore be considered conservative. A natural next step in this work is to add ice dynamics to Folgefonna for a comprehensive glacier model. This allows us to include elevation feedback as well as project total runoff and volume changes of the ice cap.

Additionally, we acknowledge that the uncertainty carried by the SMB model is high and attribute this to a few peculiarities of our calibration method. There are 559 stake measurements across Sørforonna which the calibration method tries to accommodate.



440 Firstly, the setup resolution of 100 m cannot resolve stake measurements which vary at smaller scales. Secondly, BESSIs neglected lateral processes likely play a bigger role for local differences than the entire ice cap. The calibration is potentially where including small-scale processes would yield the greatest benefits. Finally, the climate forcing used for these runs is SeNorge*. SeNorge has been proven to overestimate snow depth by about 30% for elevation ranging from 400 to 600 m a.s.l., and by 100% for elevations between 1000 and 1200 m a.s.l. (Saloranta, 2012). The dataset is still considered to yield the best estimates for snow depth in Norway, and is used to evaluate the performance of climate models such as NorCP (Lind et al., 2020). When evaluated against mass balance observations, the calibrated BESSI achieves higher accuracy than SeNorge. We could likely have further improved upon the uncertainty estimate from the calibration method if we had chosen a subset of data, i.e. by tuning BESSI to one outlet glacier. Improving upon our calibration method could therefore yield a smaller SMB model uncertainty, but lead to unwarranted confidence in its resulting projections.

5 Summary and conclusions

450 In this study, we introduce a novel analog downscaling method designed to bridge data gaps by matching high-resolution, non-transient climate models (NorCP) with transient simulations at a lower resolution (EURO-CORDEX). This computationally efficient approach enables end-users, such as glacier modelers, to produce large ensembles of physically relevant climate forcing. Consequentially, it enables SMB simulations that simultaneously account for small-scale atmospheric processes and the documented spread in plausible future climates. Here, all data are bias corrected to the western Norway region and the SMB model BESSI is calibrated using observed temperature and precipitation datasets (SeNorge) and historical mass balance measurements.

455 Applied to the Folgefonna ice cap in western Norway, our results show that future SMB evolution is strongly dependent on emission scenario. All scenarios considered (RCP2.6, 4.5, and 8.5) result in net mass loss over the 21st century, with severe degradation under RCP8.5. Midtfonna is projected to lose its accumulation zone by mid-century under all scenarios, while Nordfonna loses its accumulation zone by the end of the century under RCP4.5. The persistence of any accumulation area on Folgefonna beyond 2100 is contingent on warming remaining below RCP4.5 levels. Similarly, we find a progressively earlier spring melt with higher emission scenarios.

460 However, accounting for a plausible spread in climate model data has a substantial impact on glacier SMB and makes RCP2.6 and RCP4.5 indistinguishable from each other when considering their model spread. We find that the choice of GCM is more important for end-of-century SMB than choice of RCM. Furthermore, we theorize that the spread is mainly caused by how climate variability is represented in the climate forcing. We stress the necessity of caution when providing detailed spatial projections for mountain glaciers to affected communities. Current glaciological models can be run for spatial resolutions that far exceed resolutions of RCM ensembles. Therefore, glacier simulations that contain only a subset of plausible climate futures may give an overconfident impression of the quality of current projections. Providing faulty or lacking information to decision-makers runs the risk of fostering distrust in science when projections later prove inconsistent with observed outcomes.



Appendices

A Details on treatment of EURO-CORDEX runs

470 EURO-CORDEX has not standardized how many time steps the models contain. Both analog downscaling and BESSI require 365 day time steps, so we have done the following short cuts

- In model runs containing leap years, leap days were removed.
- In model runs with 360 day years (all models forced by HadGEM2-ES), we repeated every 72nd day of the dataset (1-Jan, 13-Mar, 25-May, 08-Aug, 19-Oct).
- 475 – One model run (MOHC-HadGEM2-ES-HadREM3-GA7-05) is missing December of 2005 in its historical run. Filled in by repeating December from 2004 instead.

Still, we excluded runs that did not have a historical run. These can be found in Table A1.

Table A1. Overview of model runs in the EURO-CORDEX ensemble that were excluded from this study.

Scenario	Driving model	Ensemble	RCM	Downscaling realisation
RCP2.6	EC-EARTH	r12i1p1	REMO2015	v1
RCP2.6	MIROC5	r1i1p1	CCLM4-8-17	v1
RCP2.6	MIROC5	r1i1p1	REMO2015	v1
RCP2.6	HadGEM2-ES	r1i1p1	REMO2015	v1
RCP4.5	HadGEM2-ES	r1i1p1	REMO2015	v1
RCP8.5	MPI-ESM-LR	r1i1p1	WRF361H	v1

B Inter-model differences: RCP2.6 and RCP4.5

Below, we display how average SMB at the end of the simulation period (2090-2100) changes with different climate forcing.
480 The same trends as discussed for RCP8.5 are visible to a large extent. HadGEM2-ES results in the most negative SMB for all three scenarios, while MPI-ESM mostly gives the most positive SMB (Fig. B1, Fig B2). For RCP4.5, CNRM-CM5 leads to higher SMB than MPI-ESM in two of four MPI-ESM model runs (Fig. B2a).

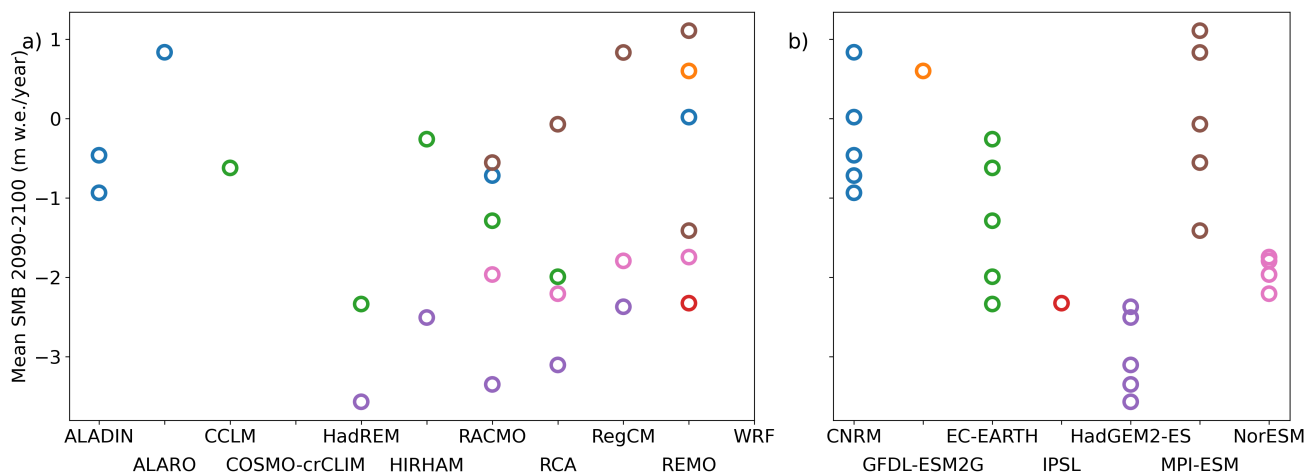


Figure B1. Same as Fig. 9, but for RCP2.6.

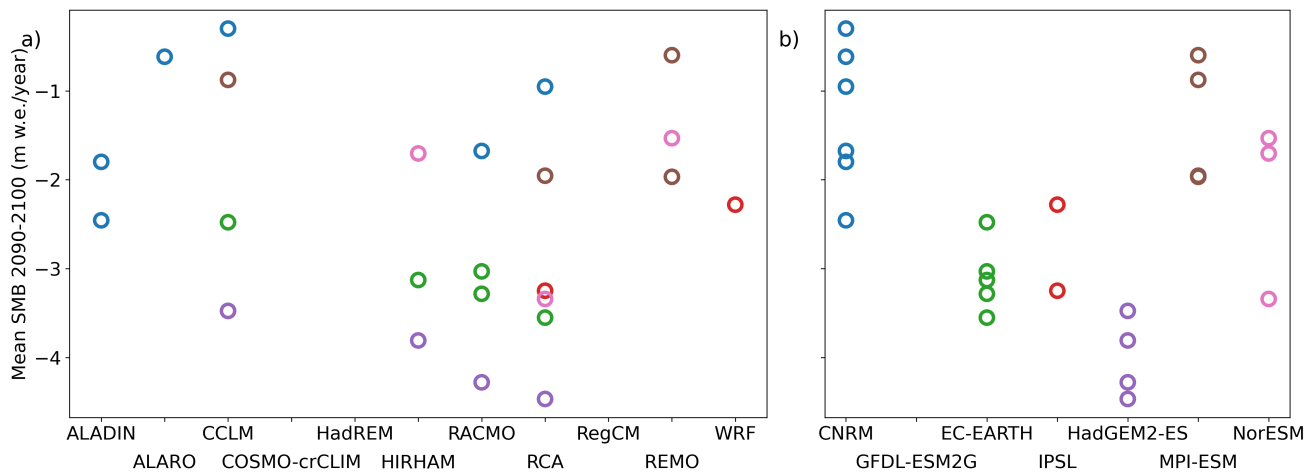


Figure B2. Same as Fig. 9, but for RCP4.5.



Author Contributions

AB and RF designed the study and developed the analog downscaling method. RF procured climate input data, set up BESSI,
485 ran and analyzed the simulations, and wrote the manuscript with input from AB.

Acknowledgements

We would like to sincerely thank Oskar Landgren at the Norwegian Meteorological Institute for valuable discussions and for
providing NorCP data. Furthermore, we thank Bjarne Kjølmoen at The Norwegian Water Resources and Energy Directorate
for providing the mass balance data from stake measurements. Generative Artificial Intelligence was occasionally used to make
490 language more concise and check spelling.

Data availability

Simulation results and analog downscaling code can be provided upon request to rebekka.froystad@uib.no.

Competing interests

The authors declare that they have no conflict of interest.



495 References

- Aguayo, R., Maussion, F., Schuster, L., Schaefer, M., Caro, A., Schmitt, P., Mackay, J., Ultee, L., Leon-Muñoz, J., and Aguayo, M.: Unravelling the sources of uncertainty in glacier runoff projections in the Patagonian Andes (40–56 S), *The Cryosphere*, 18, 5383–5406, <https://doi.org/10.5194/tc-18-5383-2024>, 2024.
- Åkesson, H., Sjurson, K. H., Vikhamar Schuler, T., Dunse, T., Andreassen, L. M., Kusk Gillespie, M., Robson, B. A., Schellenberger, T.,
500 and Clement Yde, J.: Recent history and future demise of Jostedalsgreen, the largest ice cap in mainland Europe, *The Cryosphere*, 19, 5871–5902, <https://doi.org/10.5194/tc-19-5871-2025>, 2025.
- Andreassen, L. M., Elvehøy, H., Kjøllmoen, B., Engeset, R. V., and Haakensen, N.: Glacier mass-balance and length variation in Norway, *Annals of Glaciology*, 42, 317–325, <https://doi.org/10.3189/172756405781812826>, 2005.
- Aschwanden, A., Fahnestock, M. A., Truffer, M., Brinkerhoff, D. J., Hock, R., Khroulev, C., Mottram, R., and Khan, S. A.: Contribution
505 of the Greenland Ice Sheet to sea level over the next millennium, *Science advances*, 5, eaav9396, <https://doi.org/10.1126/sciadv.aav9396>, 2019.
- Aschwanden, A., Bartholomäus, T. C., Brinkerhoff, D. J., and Truffer, M.: Brief communication: A roadmap towards credible projections of ice sheet contribution to sea level, *The Cryosphere*, 15, 5705–5715, <https://doi.org/10.5194/tc-15-5705-2021>, 2021.
- Bolibar, J., Rabatel, A., Gouttevin, I., Zekollari, H., and Galiez, C.: Nonlinear sensitivity of glacier mass balance to future climate change
510 unveiled by deep learning, *Nature Communications*, 13, 409, <https://doi.org/10.1038/s41467-022-28033-0>, 2022.
- Born, A., Imhof, M. A., and Stocker, T. F.: An efficient surface energy-mass balance model for snow and ice, *The Cryosphere*, 13, <https://doi.org/10.5194/tc-13-1529-2019>, 2019.
- Clarke, G. K., Jarosch, A. H., Anslow, F. S., Radić, V., and Menounos, B.: Projected deglaciation of western Canada in the twenty-first century, *Nature Geoscience*, 8, 372–377, <https://doi.org/10.1038/ngeo2407>, 2015.
- 515 Compagno, L., Eggs, S., Huss, M., Zekollari, H., and Farinotti, D.: Brief communication: Do 1.0, 1.5, or 2.0 °C matter for the future evolution of Alpine glaciers?, *The Cryosphere*, 15, 2593–2599, <https://doi.org/10.5194/tc-15-2593-2021>, 2021a.
- Compagno, L., Zekollari, H., Huss, M., and Farinotti, D.: Limited impact of climate forcing products on future glacier evolution in Scandinavia and Iceland, *Journal of Glaciology*, 67, 727–743, <https://doi.org/10.1017/jog.2021.24>, 2021b.
- Eidhammer, T., Booth, A., Decker, S., Li, L., Barlage, M., Gochis, D., Rasmussen, R., Melvold, K., Nesje, A., and Sobolowski, S.: Mass
520 balance and hydrological modeling of the Hardangerjøkulen ice cap in south-central Norway, *Hydrology and Earth System Sciences*, 25, 4275–4297, <https://doi.org/10.5194/hess-25-4275-2021>, 2021.
- Eklblom Johansson, F., Bakke, J., Støren, E. N., Gillespie, M. K., and Laumann, T.: Mapping of the Subglacial Topography of Folgefonna Ice Cap in Western Norway—Consequences for Ice Retreat Patterns and Hydrological Changes, *Frontiers in Earth Science*, 10, 886361, <https://doi.org/10.3389/feart.2022.886361>, 2022.
- 525 Farinotti, D.: On the effect of short-term climate variability on mountain glaciers: insights from a case study, *Journal of Glaciology*, 59, 992–1006, <https://doi.org/10.3189/2013JoG13J080>, 2013.
- Fettweis, X., Hofer, S., Krebs-Kanzow, U., Amory, C., Aoki, T., Berends, C. J., Born, A., Box, J. E., Delhasse, A., Fujita, K., Gierz, P., Goelzer, H., Hanna, E., Hashimoto, A., Huybrechts, P., Kapsch, M. L., King, M. D., Kittel, C., Lang, C., Langen, P. L., Lenaerts, J. T., Liston, G. E., Lohmann, G., Mernild, S. H., Mikolajewicz, U., Modali, K., Mottram, R. H., Niwano, M., Noël, B., Ryan, J. C., Smith, A.,
530 Streffing, J., Tedesco, M., Berg, W. J. V. D., Broeke, M. V. D., Wal, R. S. V. D., Kampenhout, L. V., Wilton, D., Wouters, B., Ziemen,



- F., and Zolles, T.: GrSMBMIP: Intercomparison of the modelled 1980-2012 surface mass balance over the Greenland Ice Sheet, *The Cryosphere*, 14, <https://doi.org/10.5194/tc-14-3935-2020>, 2020.
- Fosser, G., Khodayar, S., and Berg, P.: Benefit of convection permitting climate model simulations in the representation of convective precipitation, *Climate Dynamics*, 44, 45–60, <https://doi.org/10.1007/s00382-014-2242-1>, 2015.
- 535 Giesen, R. H. and Oerlemans, J.: Response of the ice cap Hardangerjøkulen in southern Norway to the 20th and 21st century climates, *The Cryosphere*, 4, 191–213, <https://doi.org/10.5194/tc-4-191-2010>, 2010.
- Gupta, H. V. and Kling, H.: On typical range, sensitivity, and normalization of Mean Squared Error and Nash-Sutcliffe Efficiency type metrics, *Water Resources Research*, 47, <https://doi.org/10.1029/2011WR010962>, 2011.
- Hock, R., Bliss, A., Marzeion, B., Giesen, R. H., Hirabayashi, Y., Huss, M., Radić, V., and Slangen, A. B.: GlacierMIP—A model intercompar-
540 ison of global-scale glacier mass-balance models and projections, *Journal of Glaciology*, 65, 453–467, <https://doi.org/10.1017/jog.2019.22>, 2019.
- Holube, K. M., Zolles, T., and Born, A.: Sources of uncertainty in Greenland surface mass balance in the 21st century, *The Cryosphere*, 16, 315–331, <https://doi.org/10.5194/tc-16-315-2022>, 2022.
- Hugonnet, R., McNabb, R., Berthier, E., Menounos, B., Nuth, C., Girod, L., Farinotti, D., Huss, M., Dussaillant, I., Brun, F., et al.: Accelerated
545 global glacier mass loss in the early twenty-first century, *Nature*, 592, 726–731, <https://doi.org/10.1038/s41586-021-03436-z>, 2021.
- Jacob, D., Petersen, J., Eggert, B., Alias, A., Christensen, O. B., Bouwer, L. M., Braun, A., Colette, A., Déqué, M., Georgievski, G., Georgopoulou, E., Gobiet, A., Menut, L., Nikulin, G., Haensler, A., Hempelmann, N., Jones, C., Klaus Keuler, S. K., Kröner, N., Kotlarski, S., Kriegsmann, A., Martin, E., van Meijgaard, E., Christopher Moseley, S. P., Preuschmann, S., Radermacher, C., Radtke, K., Diana Rechid, M. R., Patrick Samuelsson, S. S., Soussana, J.-F., Teichmann, C., Valentini, R., Vautard, R., Weber, B., and Yiou, P.:
550 EURO-CORDEX: new high-resolution climate change projections for European impact research, *Regional Environmental Change*, 14, 563–578, <https://doi.org/10.1007/s10113-013-0499-2>, 2014.
- Jacob, D., Teichmann, C., Sobolowski, S., Katragkou, E., Anders, I., Belda, M., Benestad, R., Boberg, F., Buonomo, E., Cardoso, R. M., et al.: Regional climate downscaling over Europe: perspectives from the EURO-CORDEX community, *Regional Environmental Change*, 20, 1–20, <https://doi.org/10.1007/s10113-020-01606-9>, 2020.
- 555 Jouvét, G. and Huss, M.: Future retreat of great Aletsch glacier, *Journal of Glaciology*, 65, 869–872, <https://doi.org/10.1017/jog.2019.52>, 2019.
- Knutti, R., Masson, D., and Gettelman, A.: Climate model genealogy: Generation CMIP5 and how we got there, *Geophysical Research Letters*, 40, 1194–1199, <https://doi.org/10.1002/grl.50256>, 2013.
- Konstali, K. and Sorteberg, A.: Why has precipitation increased in the last 120 years in Norway?, *Journal of Geophysical Research: Atmospheres*, 127, e2021JD036234, <https://doi.org/10.1029/2021JD036234>, 2022.
- 560 Kotlarski, S., Keuler, K., Christensen, O. B., Colette, A., Déqué, M., Gobiet, A., Goergen, K., Jacob, D., Lüthi, D., Van Meijgaard, E., et al.: Regional climate modeling on European scales: a joint standard evaluation of the EURO-CORDEX RCM ensemble, *Geoscientific Model Development*, 7, 1297–1333, <https://doi.org/10.5194/gmd-7-1297-2014>, 2014.
- Lind, P., Belušić, D., Christensen, O. B., Dobler, A., Kjellström, E., Landgren, O., Lindstedt, D., Matte, D., Pedersen, R. A., Toivonen, E.,
565 et al.: Benefits and added value of convection-permitting climate modeling over Fenno-Scandinavia, *Climate Dynamics*, 55, 1893–1912, <https://doi.org/10.1007/s00382-020-05359-3>, 2020.



- Lind, P., Belušić, D., Médus, E., Dobler, A., Pedersen, R. A., Wang, F., Matte, D., Kjellström, E., Landgren, O., Lindstedt, D., et al.: Climate change information over Fenno-Scandinavia produced with a convection-permitting climate model, *Climate Dynamics*, 61, 519–541, <https://doi.org/10.1007/s00382-022-06589-3>, 2023.
- 570 Lucas-Picher, P., Argüeso, D., Brisson, E., Tramblay, Y., Berg, P., Lemonsu, A., Kotlarski, S., and Caillaud, C.: Convection-permitting modeling with regional climate models: Latest developments and next steps, *Wiley Interdisciplinary Reviews: Climate Change*, 12, e731, <https://doi.org/10.1002/wcc.731>, 2021.
- Lussana, C., Saloranta, T., Skaugen, T., Magnusson, J., Tveito, O. E., and Andersen, J.: seNorge2 daily precipitation, an observational gridded dataset over Norway from 1957 to the present day, *Earth System Science Data*, 10, 235–249, <https://doi.org/10.5194/essd-10-235-2018>,
575 2018a.
- Lussana, C., Tveito, O., and Uboldi, F.: Three-dimensional spatial interpolation of 2 m temperature over Norway, *Quarterly Journal of the Royal Meteorological Society*, 144, 344–364, <https://doi.org/10.1002/qj.3208>, 2018b.
- Lussana, C., Tveito, O. E., Dobler, A., and Tunheim, K.: seNorge_2018, daily precipitation, and temperature datasets over Norway, *Earth System Science Data*, 11, 1531–1551, <https://doi.org/10.5194/essd-11-1531-2019>, 2019.
- 580 Malone, A. G., Doughty, A. M., and Macayeal, D. R.: Interannual climate variability helps define the mean state of glaciers, *Journal of Glaciology*, 65, 508–517, 2019.
- Maraun, D.: Nonstationarities of regional climate model biases in European seasonal mean temperature and precipitation sums, *Geophysical Research Letters*, 39, <https://doi.org/10.1029/2012GL051210>, 2012.
- Marzeion, B., Hock, R., Anderson, B., Bliss, A., Champollion, N., Fujita, K., Huss, M., Immerzeel, W. W., Kraaijenbrink, P., Malles, J.-H., et al.: Partitioning the uncertainty of ensemble projections of global glacier mass change, *Earth's Future*, 8, e2019EF001470, <https://doi.org/10.1029/2019EF001470>, 2020.
- Masson, D. and Knutti, R.: Climate model genealogy, *Geophysical Research Letters*, 38, <https://doi.org/10.1029/2011GL046864>, 2011.
- McKay, M. D., Beckman, R. J., and and, W. J. C.: A Comparison of Three Methods for Selecting Values of Input Variables in the Analysis of Output From a Computer Code, *Technometrics*, 42, 55–61, <https://doi.org/10.1080/00401706.2000.10485979>, 2000.
- 590 Médus, E., Thomassen, E. D., Belušić, D., Lind, P., Berg, P., Christensen, J. H., Christensen, O. B., Dobler, A., Kjellström, E., Olsson, J., et al.: Characteristics of precipitation extremes over the Nordic region: added value of convection-permitting modeling, *Natural Hazards and Earth System Sciences*, 22, 693–711, <https://doi.org/10.5194/nhess-22-693-2022>, 2022.
- Mikkelsen, T. B., Grinsted, A., and Ditlevsen, P.: Influence of temperature fluctuations on equilibrium ice sheet volume, *The Cryosphere*, 12, 39–47, <https://doi.org/10.5194/tc-12-39-2018>, 2018.
- 595 Milner, A. M., Khamis, K., Battin, T. J., Brittain, J. E., Barrand, N. E., Füreder, L., Cauvy-Fraunié, S., Gíslason, G. M., Jacobsen, D., Hannah, D. M., et al.: Glacier shrinkage driving global changes in downstream systems, *Proceedings of the National Academy of Sciences*, 114, 9770–9778, <https://doi.org/10.1073/pnas.1619807114>, 2017.
- Nash, J. E. and Sutcliffe, J. V.: River flow forecasting through conceptual models part I—A discussion of principles, *Journal of Hydrology*, 10, 282–290, [https://doi.org/10.1016/0022-1694\(70\)90255-6](https://doi.org/10.1016/0022-1694(70)90255-6), 1970.
- 600 Nesje, A.: Future state of Norwegian glaciers: Estimating glacier mass balance and equilibrium line responses to projected 21st century climate change, *The Holocene*, 33, 1257–1271, <https://doi.org/10.1177/09596836231183069>, 2023.
- Nesje, A., Bakke, J., Dahl, S. O., Lie, Ø., and Matthews, J. A.: Norwegian mountain glaciers in the past, present and future, *Global and Planetary Change*, 60, 10–27, <https://doi.org/10.1016/j.gloplacha.2006.08.004>, 2008.
- Perrette, M.: Latin hypercube sampling, <https://github.com/perrette/runner>, 2013.



- 605 Pontoppidan, M., Reuder, J., Mayer, S., and Kolstad, E. W.: Downscaling an intense precipitation event in complex terrain: the importance of high grid resolution, *Tellus A: Dynamic Meteorology and Oceanography*, <https://doi.org/10.1080/16000870.2016.1271561>, 2017.
- Qian, Y., Jackson, C., Giorgi, F., Booth, B., Duan, Q., Forest, C., Higdon, D., Hou, Z. J., and Huerta, G.: Uncertainty quantification in climate modeling and projection, *Bulletin of the American Meteorological Society*, 97, 821–824, <https://doi.org/10.1175/BAMS-D-15-00297.1>, 2016.
- 610 Radić, V., Bliss, A., Beedlow, A. C., Hock, R., Miles, E., and Cogley, J. G.: Regional and global projections of twenty-first century glacier mass changes in response to climate scenarios from global climate models, *Climate Dynamics*, 42, 37–58, <https://doi.org/10.1007/s00382-013-1719-7>, 2014.
- Reichert, B. K., Bengtsson, L., and Oerlemans, J.: Recent glacier retreat exceeds internal variability, *Journal of Climate*, 15, 3069–3081, [https://doi.org/10.1175/1520-0442\(2002\)015<3069:RGREIV>2.0.CO;2](https://doi.org/10.1175/1520-0442(2002)015<3069:RGREIV>2.0.CO;2), 2002.
- 615 Rounce, D. R., Hock, R., Maussion, F., Hugonnet, R., Kochtitzky, W., Huss, M., Berthier, E., Brinkerhoff, D., Compagno, L., Copland, L., et al.: Global glacier change in the 21st century: Every increase in temperature matters, *Science*, 379, 78–83, <https://doi.org/10.1126/science.abo1324>, 2023.
- Saloranta, T.: Simulating snow maps for Norway: description and statistical evaluation of the seNorge snow model, *The Cryosphere*, 6, 1323–1337, <https://doi.org/10.5194/tc-6-1323-2012>, 2012.
- 620 Schmidt, L., Aðalgeirsdóttir, G., Pálsson, F., Langen, P., Guðmundsson, S., and Björnsson, H.: Dynamic simulations of Vatnajökull ice cap from 1980 to 2300, *Journal of Glaciology*, 66, 97–112, <https://doi.org/10.1017/jog.2019.90>, 2020.
- Tebaldi, C., Debeire, K., Eyring, V., Fischer, E., Fyfe, J., Friedlingstein, P., Knutti, R., Lowe, J., O'Neill, B., Sanderson, B., et al.: Climate model projections from the scenario model intercomparison project (ScenarioMIP) of CMIP6, *Earth System Dynamics*, 12, 253–293, <https://doi.org/10.5194/esd-12-253-2021>, 2021.
- 625 Thornton, P. K., Ericksen, P. J., Herrero, M., and Challinor, A. J.: Climate variability and vulnerability to climate change: a review, *Global Change Biology*, 20, 3313–3328, <https://doi.org/10.1111/gcb.12581>, 2014.
- Vautard, R., Kadyrov, N., Iles, C., Boberg, F., Buonomo, E., Bülow, K., Coppola, E., Corre, L., van Meijgaard, E., Nogherotto, R., Sandstad, M., Schwingshackl, C., Somot, S., Aalbers, E., Christensen, O. B., Ciarlo, J. M., Demory, M.-E., Giorgi, F., Jacob, D., Jones, R. G., Keuler, K., Kjellström, E., Lenderink, G., Levvasseur, G., Nikulin, G., Sillmann, J., Solidoro, C., Sørland, S. L., Steger, C., Teichmann, C., Warrach-Sagi, K., and Wulfmeyer, V.: Evaluation of the Large EURO-CORDEX Regional Climate Model Ensemble, *Journal of Geophysical Research: Atmospheres*, 126, <https://doi.org/https://doi.org/10.1029/2019JD032344>, 2021.
- 630 Viviroli, D., Archer, D. R., Buytaert, W., Fowler, H. J., Greenwood, G. B., Hamlet, A. F., Huang, Y., Koboltschnig, G., Litaor, M., López-Moreno, J. I., et al.: Climate change and mountain water resources: overview and recommendations for research, management and policy, *Hydrology and Earth System Sciences*, 15, 471–504, <https://doi.org/10.5194/hess-15-471-2011>, 2011.
- 635 Weathers, M., Rounce, D. R., Fasullo, J., and Maussion, F.: Evaluating the role of internal climate variability and bias adjustment methods on decadal glacier projections, *Earth's Future*, 13, e2024EF005624, <https://doi.org/10.1029/2024EF005624>, 2025.
- Zekollari, H., Huss, M., and Farinotti, D.: Modelling the future evolution of glaciers in the European Alps under the EURO-CORDEX RCM ensemble, *The Cryosphere*, 13, 1125–1146, <https://doi.org/10.5194/tc-13-1125-2019>, 2019.
- Zekollari, H., Huss, M., Farinotti, D., and Lhermitte, S.: Ice-dynamical glacier evolution modeling—A review, *Reviews of Geophysics*, 60, e2021RG000754, <https://doi.org/10.1029/2021RG000754>, 2022.
- 640 Zolles, T. and Born, A.: Sensitivity of the Greenland surface mass and energy balance to uncertainties in key model parameters, *The Cryosphere*, 15, 2917–2938, <https://doi.org/10.5194/tc-15-2917-2021>, 2021.

<https://doi.org/10.5194/egusphere-2026-1090>

Preprint. Discussion started: 24 March 2026

© Author(s) 2026. CC BY 4.0 License.



Zolles, T. and Born, A.: How does a change in climate variability impact the Greenland ice sheet surface mass balance?, *The Cryosphere*, 18, 4831–4844, <https://doi.org/10.5194/tc-18-4831-2024>, 2024.

645 Åkesson, H., Nisancioglu, K. H., Giesen, R. H., and Morlighem, M.: Simulating the evolution of Hardangerjøkulen ice cap in southern Norway since the mid-Holocene and its sensitivity to climate change, *The Cryosphere*, 11, <https://doi.org/10.5194/tc-11-281-2017>, 2017.